Balanced pure carving turns in alpine skiing

Serguei S. Komissarov

Department of Applied Mathematics

The University of Leeds

Leeds, LS2 9JT, UK

Abstract

In this paper we analyse the model of pure carving turns in alpine skiing and snowboarding based on the usual assumption of approximate balance between forces and torques acting on the skier during the turn. The approximation of torque balance yields both lower and upper limits on the skier speed, which depend only on the sidecut radius of skis and the slope gradient. We use the model to simulate carving runs on slopes of constant gradient and find that pure carving is possible only on slopes of relatively small gradient, with the critical slope angle in the range of $8° - 20°$. The exact value depends mostly on the coefficient of snow friction and to a lesser degree on the sidecut radius of skis. Comparison with the practice of ski racing shows that the upper speed limit and the related upper limit on the slope gradient set by the model are too restrictive and so must be the assumption of torque balance used in the model. A more advanced theory is needed.

Keywords: alpine skiing, modelling, balance/stability, performance

Introduction

When making their way down the hill, expert skiers execute complex coordinated body movements, often within a fraction of a second, which allow them to ski at speed and yet to remain in control. Their decisions are dictated by many factors, such as terrain, snow condition, equipment, etc. A ski racer faces additional challenges as a race course significantly reduces the freedom of choosing trajectory. There is a great deal of qualitative understanding of skiing techniques and race tactics based on the personal experiences of ski professionals, coaches and instructors (e.g. LeMaster, 2010). However, this empirical knowledge is imprecise, very subjective and sometimes even subconscious, and this keeps the door open to misunderstanding, misconceptions and controversies.

Scientific approach can help to put the understanding of skiing on a more solid footing by using the well-tested basic principles of mechanics (including biomechanics) and exploring various aspects of physical interactions specific to skiing. In fact, there has already been a great deal of research in this area and a large number of interesting results can be found in various journals dedicated to sport, medicine, physics, engineering, etc. Basic theoretical principles are summarised in several monographs (e.g. Howe, 1983; Lind & Sanders, 1996). Although a significant progress has been made, we are still far from the point where researches can declare a complete understanding of the topic and provide a clear guidance to skiing enthusiasts and professionals. The main problem is that a skier and their equipment is a very complicated mechanical system with many degrees of freedom. In order to arrive to a treatable and comprehensible mathematical model, a great deal of simplification is required.

The most basic approach is to treat the skier as a point mass moving under the action of the gravitational force, the snow reaction forces and the aerodynamic drag (Howe, 1983; Lind & Sanders, 1996). The snow reaction force is known to depend on the angle between the longitudinal axis of skis and their direction of motion, the so-called angle of attack. For example in order to brake and stop, skis are routinely pivoted to the angle of attack about 90°. This force also depends on whether skis are flat on the snow or put at an angle with to it, called the edge angle. For example in order to halt side-slipping down the fall line, skiers increase the edge angle by increasing inclination of their body to the slope and/or its angulation. The inclination angle is also important for the lateral balance of skiers as deviation from the balanced inclination may result in a fall. In fact, in mathematical modelling of skiing it is commonly assumed that during straight runs, traversed runs, and even turns, skier's body is in lateral balance. This dictates the position of their centre of mass (CM) over the skis and hence allows to introduce the ski edge angle into the dynamics of point mass (Howe, 1983; Lind & Sanders, 1996).

At the over extreme we find more complex Hanavan-like models of skiers and their equipment, where they are represented by many rigid segments connected by mechanical joints (Oberegger, Kaps, Mössner, Heinrich, & Nachbauer, 2010). While this approach is undoubtedly very useful in studying the ski-snow interaction (P. Federolf, Roos, Lüthi, & Dual, 2010; Mössner, Heinrich, Kaps, Schretter, & Nachbauer, 2008; Mössner, Heinrich, Kaps, Schretter, & Nachbauer, 2009; Mössner et al., 2006), the biomechanical response of a human body is very complex a hence very difficult to model accurately. It requires a significant element of artificial intelligence. Undoubtedly, this is the future of computer modelling of skiing, but at the moment more basic models allowing simple interpretation and clear insights into the key factors of skiing dynamics seem more appropriate.

The apparently lesser problem of the interaction between skis and snow is also complicated, and not only due to the non-trivial ski construction but also due to the existence of many different types of snow with their complex structure and physics.

Even for straight gliding one has to differentiate between the so-called dry friction, which arises in the case of direct contact of the ski base with the snow, and the wet friction, which arises due to meltwater lubrication of the ski base (e.g. Colbeck, 1992; Nachbauer, Kaps, Hasler, & Mössner, 2016). In soft fresh snow and slush, the processes of snow compactification and plowing can be the dominant contributors to effective friction (e.g. Colbeck, 1992). On hard snow typical for machine-prepared pistes and race tracks, the snow-ski-edge interaction becomes important. This interaction may be analogous to that between a sharp hardened tool and a workpiece in machining operations (Brown, 2009; Merchant, 1945; Tada & Hirano, 2002). Indeed, ski racers meticulously keep the edges of their skis razor-sharp.

A modern generic ski turn is hybrid in nature. It is initiated with pivoting skis towards the new turn direction and skidding, and it is finished as carving (e.g. LeMaster, 2010; Reid, 2010; Spörri, Kröll, Gildien, & Müller, 2016). At one extreme end of the distribution of hybrid turns, we have a pure skidded (or steered) turn, where a significant angle of attack is preserved from start to finish. The turning action of this turn arises due to the component of the snow reaction force which is normal to the direction of motion (Hirano, 2006; Nordt, Springer, & Kollár, 1999; Tada & Hirano, 2002). At the other extreme, we find a pure carved turn, where the angle of attack is almost zero and each ski moves along a curved groove it cuts in the snow. The groove curvature is determined by the geometry of the ski edge and the ski edge angle (Howe, 1983; Lind & Sanders, 1996). A simple way of determining the composition of a hybrid turn is via naked eye inspection of the tracks left by the skis on the snow. Where the tracks are wide, the turn is skidded, and where they are narrow, it is carved. The closer tracks are to narrow lines from start to finish the closer the turn is to a purely carved one. In terms of performance, the main advantage of carved turns is significant reduction of energy dissipation and hence increased speed.

The advance of modern highly shaped skis has moved the focus of both competitive and high-performance recreational skiing from steered to carved turns. Nowadays even mass-produced skis are shaped, thus giving the opportunity to enjoy carving runs to all skiing enthusiasts. This has even made an impact on the way the alpine skiing is taught by some ski instructors, who now teach how to initiate a new turn not via pivoting but by rolling skis from edge to edge (e.g. Harb, 2006).

The dynamics of carving turns has already received significant attention in the theory of skiing (Howe, 1983; Jentschura & Fahrbach, 2004; Lind & Sanders, 1996). Naively, one may think that skiers can change the edge angle of their skis at will and hence fully control the local shape (curvature) of their trajectory. However, this is not quite the case because the edge angle in largely dictated by the inclination angle of the skier, which is also an important parameter for skier's lateral balance. For example, a stationary skier must stay more-or-less vertical to avoid falling to the one side or the other. If their whole body is aligned (or "stacked") with the vertical direction then the ski edge angle equals the angle of the slope gradient. If their body is angulated

at their knees or hip, while keeping the CM above the skis, the edge angle is different but this variation is limited in amplitude. A similar analysis of skier's balance during pure carving turns allows to derive a relatively simple equation which relates the edge angle and hence the local curvature of skier's trajectory with their speed and direction of motion relative to the fall line (Howe, 1983; Jentschura & Fahrbach, 2004; Lind & Sanders, 1996). This so-called Ideal Carving Equation (ICE) removes the need for specifying the component of the snow reaction force responsible for the turning action, which is a significant gain. As a result, the motion of skiers's CM can be fully determined in a model where only the gravity, dynamic friction and air resistance forces are explicitly taken into account.

Testing the hypothesis that this simplified model adequately describes the dynamics of carving turns is the main topic of this paper. In particular, Jentschura and Fahrbach (2004) discovered an upper limit on the skier speed imposed by ICE. They concluded that in slalom races the typical speed is below this limit and considered this as a justification of the model. By calculating the actual motion of a skier as governed by this model, one can trace the evolution of their speed and check the conditions under which it stays below the limit. This can be done not only for slalom but also for other race disciplines.

Methods

The characteristic scales of fall-line gliding

Although recreational skiing can be very relaxed and performance skiing physically most demanding, the dominant source of energy in both cases is the Earth's gravity. The total available gravitational energy is

$$U = mgh \,, \tag{1}$$

where m is skier's mass, g is the gravitational acceleration and h is the total vertical drop of the slope. If all this energy was converted into the kinetic energy of the skier, $K = mv^2/2$, then at the bottom of the slope the speed would reach

$$v = \sqrt{2gh} \approx 227 \left(\frac{h}{200\,\mathrm{m}} \right)^{1/2} \mathrm{km/h} \,. \tag{2}$$

Although this not far from what is achieved in the speed skiing competitions where skiers glide straight down the fall line, the typical speeds in other alpine disciplines are significantly lower, indicating there are some forces working against gravity. Two of the candidates are the dynamic snow friction and the aerodynamic drag (Lind & Sanders, 1996).

The friction force is antiparallel to the skier velocity vector $\boldsymbol{v}$ and its magnitude relates to the normal reaction force $\boldsymbol{F}_\mathrm{n}$. Although the physics of snow friction is quite complicated (e.g. Lind & Sanders, 1996), the basic Coulomb equation

$$F_\mathrm{f} = \mu F_\mathrm{n} \,, \tag{3}$$

is almost universally used both in describing the results of field studies and in modelling of ski runs (e.g. Lind & Sanders, 1996; Mössner et al., 2008; Nachbauer et al., 2016; Rudakov, Lisovski, Ilyalov, & Podgaets, 2010). The dynamic coefficient of friction μ depends on many factors, e.g. snow temperature, wax used and even the value of F_n, making the relation between F_f and F_n nonlinear (e.g. Nachbauer et al., 2016). Sometimes, even the effect of snowplowing in a skidded turn is described using the Coulomb law (Sahashi & Ichino, 1998), leading to very high values of the coefficient $\mu \leq 0.3$. For the purpose of our study it is sufficient to use constant μ and to address how its value affects the outcome of simulations.

In the case of gliding down the fall line

$$F_\mathrm{n} = mg \cos \alpha \,, \tag{4}$$

where α is the angle between the slope and the horizontal plane. Because the friction force does not depend on the skier's speed, it cannot limit the speed but only reduces its growth rate. The aerodynamic drag force is also antiparallel to the velocity vector and has the magnitude

$$F_\mathrm{d} = \kappa v^2 \quad \text{where} \quad \kappa = \frac{C_\mathrm{d} A \rho}{2} \,, \tag{5}$$

where C_d is the drag coefficient, A is the cross-section area of the skier normal to the direction of motion and ρ is the mass density of the air (Lind & Sanders, 1996). The drag force grows with v and this results in speed saturation. The value of the saturation speed v_s can be easily found from the energy principle. At this speed, the work carried out by the drag and friction forces over the distance L along the fall line,

$$W = (F_\mathrm{f} + F_\mathrm{d})L \,, \tag{6}$$

must be equal to the gravitational energy $U = mgh$ released over the same distance. This condition yields

$$v_\mathrm{s}^2 = \frac{mg}{\kappa} \sin \alpha (1 - \mu \cot \alpha) \tag{7}$$

(cf. Lind and Sanders (1996)). Incidentally, this result shows that the slope angle has to exceed $\alpha_\mathrm{min} = \arctan(\mu)$. For the realistic value $\mu = 0.04$ (Lind & Sanders, 1996), this gives $\alpha_\mathrm{min} = 2.3^o$. Usually ski slopes are significantly steeper than this and the snow friction contribution is small. In this case, the saturation speed is determined mostly by the balance between the gravity and aerodynamic drag, which yields the characteristic speed scale

$$V_\mathrm{g} = \sqrt{\frac{mg}{\kappa} \sin \alpha} \,. \tag{8}$$

The time required to reach this speed under the action of gravity alone,

$$T_\mathrm{g} = \frac{V_\mathrm{g}}{g \sin \alpha} = \sqrt{\frac{m}{\kappa g \sin \alpha}} \,, \tag{9}$$

is the corresponding characteristic time scale. The length scale

$$L_{\mathrm{g}} = \frac{V_{\mathrm{g}}T_{\mathrm{g}}}{2} = \frac{m}{2\kappa} \tag{10}$$

is the corresponding distance along the slope. Interestingly, L_{g} does not depend on the slope gradient, which may not be very intuitive. Lind and Sanders (1996) state the values $C_{\mathrm{d}} = 0.5$, $m = 80\,\mathrm{kg}$, $A = 0.4\,\mathrm{m}^2$, and $\rho = 1.2\,\mathrm{kg/m}^3$ as typical for downhill (DH) competitions. For these parameters

$$V_{\mathrm{g}} \simeq 150\sqrt{\frac{\sin\alpha}{\sin 15°}}\,\mathrm{km/h}\,, \quad T_{\mathrm{g}} \simeq 16\sqrt{\frac{\sin 15°}{\sin\alpha}}\,\mathrm{s}\,, \quad L_{\mathrm{g}} \simeq 0.33\,\mathrm{km}\,. \tag{11}$$

These scales are well below the lengths of race tracks and durations of ski runs in all alpine disciplines, suggesting that V_g can be reached in all of them. For example, the length of Kitzbuhel's famous DH track Streif is 3.3km ($\langle\alpha\rangle = 15°$) and the length of it slalom track Ganslern is 0.59km ($\langle\alpha\rangle = 19°$) (www.hahnenkamm.com). Although on some sections of downhill (DH) courses the skier speed can indeed approach V_g, with the current record of 162 km/h belonging to Johan Clarey (FIS WC race in Wengen, 2013), the typical mean speed in DH is $\langle v\rangle \simeq 90\,\mathrm{km/h}$, which is significantly lower than V_g (e.g. Gilgien, Spörri, Kröll, Crivelli, & Müller, 2014). In slalom (SL) it stays well below, only $40 - 50\,\mathrm{km/h}$ (e.g. Reid, 2010; Supej, Hebert-Losier, & Holmberg, 2014), indicating that the applicability of the fall-line gliding model is rather limited. In equation (11) we used $\alpha = 15°$ as a typical mean gradient of red slopes. On steeper slopes, the limitation of the model is even more pronounced.

Basic dynamics of alpine skiing

Here we limit ourselves to the idealised case of a plane slope with constant gradient and introduce such system of Cartesian coordinates $\{x, y, z\}$ associated with the slope that on its surface $z = 0$. The unit vectors parallel to the coordinate axes will be denoted as $\{\boldsymbol{i}, \boldsymbol{j}, \boldsymbol{k}\}$ respectively. For convenience, we direct the y-axis along the fall line, pointing downhill. We also introduce the vertical unit vector $\boldsymbol{s} = -\sin(\alpha)\boldsymbol{j} + \cos(\alpha)\boldsymbol{k}$, so that the gravitational acceleration $\boldsymbol{g} = -g\boldsymbol{s}$ (see figure 1).

When only the gravity, normal reaction, dynamic friction and aerodynamic drag forces are taken into account, the second law of Newtonian mechanics governing the motion of skier's centre of mass (CM) reads

$$m\frac{d\boldsymbol{v}}{dt} = \boldsymbol{F}_{\mathrm{g}} + \boldsymbol{F}_{\mathrm{f}} + \boldsymbol{F}_{\mathrm{d}} + \boldsymbol{F}_{\mathrm{n}}\,, \tag{12}$$

where

$$\boldsymbol{F}_{\mathrm{g}} = m\boldsymbol{g}\,, \quad \boldsymbol{F}_{\mathrm{f}} = -\mu F_{\mathrm{n}}\boldsymbol{u}\,, \quad \boldsymbol{F}_{\mathrm{d}} = -kv^2\boldsymbol{u} \tag{13}$$
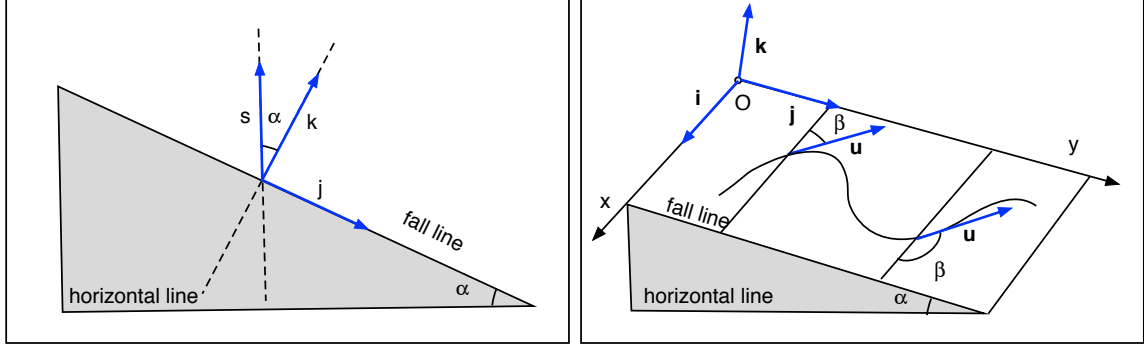
Figure 1. Geometry of the slope. *Left panel:* The vertical section of the slope along the fall line. *Right panel:* The slope as seen at an angle from above. The curved line in the middle is the skier trajectory.

are the total gravity, friction, aerodynamic drag, and snow reaction force acting on the skier, respectively, and $\boldsymbol{F}_{\mathrm{n}}$ is the normal reaction. In these expressions, $\boldsymbol{u}$ is the unit vector in the direction of motion. It is convenient to introduce the *angle of traverse* β as the angle between $-\boldsymbol{i}$ and $\boldsymbol{u}$ for the right turns and between $\boldsymbol{i}$ and $\boldsymbol{u}$ for the left turns of a run (see figure 1). With this definition,

$$\boldsymbol{u} = \mp\cos(\beta)\boldsymbol{i} + \sin(\beta)\boldsymbol{j} \tag{14}$$

where the upper sign of $\cos\beta$ corresponds to the right turns and the lower sign to the left turns (we will use this convention throughout the paper).

The normal reaction force $\boldsymbol{F}_{\mathrm{n}}$ is not as easy to describe as the other forces. First, unless the skis are running flat on the slope, this force is normal not to the slope surface but to the contact surface between the snow and the skis, which is not the same thing. When skis are put on edge, they carve a platform (or a step) in the snow and the normal reaction force is normal to the surface (surfaces) of this platform (LeMaster, 2010). Second, the effective weight of the skier is determined not only by the gravity but also by the centrifugal force, which depends on the skier speed and the local curvature of their trajectory.

Since the velocity vector $\boldsymbol{v} = v\boldsymbol{u}$ we have

$$\frac{d\boldsymbol{v}}{dt} = \boldsymbol{u}\frac{dv}{dt} + v\frac{d\boldsymbol{u}}{dt}\,. \tag{15}$$

Ignoring the up and down motion of CM, we can write $d\boldsymbol{u}/dt = \boldsymbol{c}|d\beta/dt|$, where $\boldsymbol{c}$ is the centripetal unit vector which points towards the local centre of curvature of the CM trajectory. Hence,

$$\frac{d\boldsymbol{v}}{dt} = \boldsymbol{u}\frac{dv}{dt} + v\boldsymbol{c}\left|\frac{d\beta}{dt}\right|\,. \tag{16}$$

214 Since $dt = dl/v$, where l is the distance measured along the skier trajectory, the last
215 equation can also be written as

$$\frac{d\boldsymbol{v}}{dt} = \boldsymbol{u}\frac{dv}{dt} + \frac{v^2}{R}\boldsymbol{c}\,, \tag{17}$$

216 where

$$R = \left|\frac{dl}{d\beta}\right| \tag{18}$$

217 is the (local) radius of curvature of the trajectory. Hence, we can rewrite equation
218 (12) as

$$m\boldsymbol{u}\frac{dv}{dt} + \frac{mv^2}{R}\boldsymbol{c} = \boldsymbol{F}_{\mathrm{g}} + \boldsymbol{F}_{\mathrm{f}} + \boldsymbol{F}_{\mathrm{d}} + \boldsymbol{F}_{\mathrm{n}}\,. \tag{19}$$

219   Scalar multiplication of equation (19) with $\boldsymbol{u}$ delivers the equation governing
220 the evolution of skier's speed. Since $\boldsymbol{u} \cdot \boldsymbol{c} = 0\,, \quad \boldsymbol{u} \cdot \boldsymbol{u} = 1\,, \quad \boldsymbol{u} \cdot \boldsymbol{s} = -\sin\alpha\sin\beta,$
221 this equation reads

$$\frac{dv}{dt} = g\sin\alpha\sin\beta - \mu\frac{F_{\mathrm{n}}}{m} - \frac{k}{m}v^2\,. \tag{20}$$

222   The normal reaction force can be decomposed into components parallel to $\boldsymbol{c}$ and
223 $\boldsymbol{k}$:

$$\boldsymbol{F}_{\mathrm{n}} = F_{\mathrm{n,c}}\boldsymbol{c} + F_{\mathrm{n,k}}\boldsymbol{k}\,. \tag{21}$$

224 The scalar multiplication of equation (19) and $\boldsymbol{k}$ immediately yields

$$F_{\mathrm{n,k}} = mg\cos\alpha\,. \tag{22}$$

225 Thus, the normal to the slope component of the snow reaction force $\boldsymbol{F}_{\mathrm{n}}$ is the same
226 as in the case of the fall-line gliding. This is what is needed to match exactly the
227 normal to the slope component of the gravity force and hence to keep the skier on
228 the slope.
229   Since $\boldsymbol{c} = \pm\sin(\beta)\boldsymbol{i} + \cos(\beta)\boldsymbol{j}$, (see figure 2) and hence $(\boldsymbol{s}\cdot\boldsymbol{c}) = -\sin\alpha\cos\beta,$
230 the scalar multiplication of equation (19) with $\boldsymbol{c}$ yields

$$F_{\mathrm{n,c}} = \frac{mv^2}{R} - mg\sin\alpha\cos\beta\,. \tag{23}$$

231 This component of the normal reaction force is stronger in the lower-c part of the
232 turn ($90° < \beta < 180°$), where the angle between the gravity force and the centrifugal
233 force is less than 90°, and weaker in the upper-c part of the turn ($0° < \beta < 90°$),
234 where this angle is more than 90° (the terminology is from Harb (2006)).
235   The total strength of $\boldsymbol{F}_{\mathrm{n}}$ (and hence the effective weight of the skier) is

$$F_{\mathrm{n}} = \frac{mg\cos\alpha}{\cos\Phi}\,, \tag{24}$$
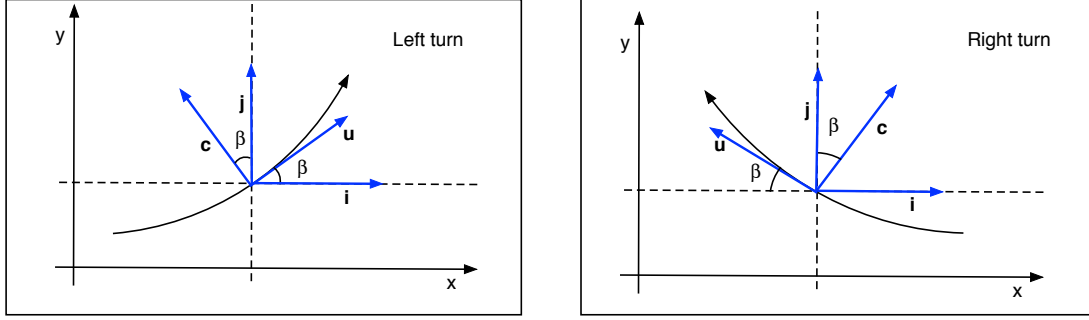
Figure 2. The centripetal unit vector $\boldsymbol{c}$ for left and right turns.

where Φ is the angle between $\boldsymbol{F}_{\mathrm{n}}$ and the normal direction to the slope $\boldsymbol{k}$, given by

$$\tan\Phi = \frac{F_{\mathrm{n,c}}}{F_{\mathrm{n,k}}} = \frac{v^2}{gR}\frac{1}{\cos\alpha} - \tan\alpha\cos\beta\,. \tag{25}$$

In the case of fall-line gliding, $\Phi = 0°$ and this equation reduces to the familiar $F_{\mathrm{n}} = mg\cos\alpha$, as expected.

Formally, equations (22,23) can be written as one vector equation

$$\boldsymbol{F}_{\mathrm{n}} + \boldsymbol{F}_{\mathrm{c}} + \boldsymbol{F}_{\mathrm{g,lat}} = 0\,, \tag{26}$$

where

$$\boldsymbol{F}_{\mathrm{g,lat}} = -(mg\cos\alpha)\boldsymbol{k} + (mg\sin\alpha\cos\beta)\boldsymbol{c} \tag{27}$$

is the lateral (normal to $\boldsymbol{u}$) component of the gravity force and

$$\boldsymbol{F}_{\mathrm{c}} = -(mv^2/R)\boldsymbol{c} \tag{28}$$

is the centrifugal force. Equation (26) also holds in the accelerated (non-inertial) frame of the skier where $\boldsymbol{F}_{\mathrm{c}}$ emerges as an inertial force. In this frame, the skier is at rest and equation (26) has the meaning of lateral force balance. As any inertial force, the centrifugal force has the same properties as the gravity force and their sum plays the role of effective gravity experienced by the skier. Introducing the lateral effective gravity

$$\boldsymbol{F}_{\mathrm{g,eff}} = \boldsymbol{F}_{\mathrm{g,lat}} + \boldsymbol{F}_{\mathrm{c}}\,, \tag{29}$$

equation (26) can be written as

$$\boldsymbol{F}_{\mathrm{n}} + \boldsymbol{F}_{\mathrm{g,eff}} = 0\,. \tag{30}$$

The effective weight F_{n} is often measured in the units of the standard weight mg, in which case it is also called the g-force. Using equation (24), we find

$$\text{g-force} = \frac{\cos\alpha}{\cos\Phi}\,. \tag{31}$$

The expressions (24,25) for the strength and direction of $\boldsymbol{F}_{\mathrm{n}}$ do not allow to close the system. Indeed, they involve the turn radius R which still remains undetermined.

Radius of balanced carving turn

In the mechanics of solid bodies, by a balance we understand not only vanishing combined (total) force but also vanishing combined torque (Landau & Lifshitz, 1969). Although skiers are not exactly solid bodies, torques are still important in their dynamics. Here we focus on the lateral balance of skiers, that is the balance in the plane normal to the skier speed (the so-called frontal plane; LeMaster, 2010). The two forces parallel to this plane are the effective gravity $\boldsymbol{F}_{\mathrm{g,eff}}$ and the normal reaction $\boldsymbol{F}_{\mathrm{n}}$. The effective gravity is applied directly at the CM, whereas the normal reaction force is applied at the skis and most of it originates from the inside edge of the outside (relative to the turn arc) ski (LeMaster, 2010). Hence, the condition of vanishing torque implies that both $\boldsymbol{F}_{\mathrm{g,eff}}$ and $\boldsymbol{F}_{\mathrm{n}}$ must act along the line connecting CM with the inside edge of the outside ski (see figure 3). In other words, the angle between this line, which we will refer to as the lever arm, and the slope normal, which is called the skier inclination angle, must be equal to the angle Φ given by equation (25).

As a first step, here we focus on the case where the skier is "stacked", which means that in the frontal plane their legs are aligned with their torso in the frontal plane. In this case, skier's CM is located about their belly button and the lever arm is normal to the ski base, provided skier's boots are properly adjusted (the so-called canting of ski boots; LeMaster, 2010). Hence, the angle Ψ between the ski base and the slope, which we will call the ski edge angle (see figure 3), equals the skier inclination angle

$$\Psi = \Phi \,. \tag{32}$$

The running edge of a flattened carving ski is close to an arc of a circle. The radius of this circle is called the ski sidecut radius, R_{sc}. When the ski is placed at the edge angle Ψ to a hard flat surface and then pressed in the middle so it bends and comes into contact with the surface, its edge can still be approximated as an arc but of a smaller radius

$$R_{\mathrm{e}} = R_{\mathrm{sc}} \cos \Psi \tag{33}$$

(Howe (1983), Lind and Sanders (1996), and Appendix A). In pure carving turns, there is no side-slippage (skidding) and the ski is transported along the contact edge. This makes the edge curvature radius R_{e} the same as the local curvature radius of the ski trajectory.

Strictly speaking, this relation is based on the assumption that the penetration of snow surface by skis is negligibly small, which is best satisfied on an icy race track. If however the snow is soft, and hence the penetration is significant, it is important to know how the penetration depth is distributed along the ski. As the pressure distribution normally peaks under skier's foot, one may expect the penetration to be deepest near the ski midpoint. Assuming that both the tip and the tail ends of the running edge remain on the surface, Howe (1983) derived a modified version of equation (33), which includes the penetration depth as a parameter and leads to a
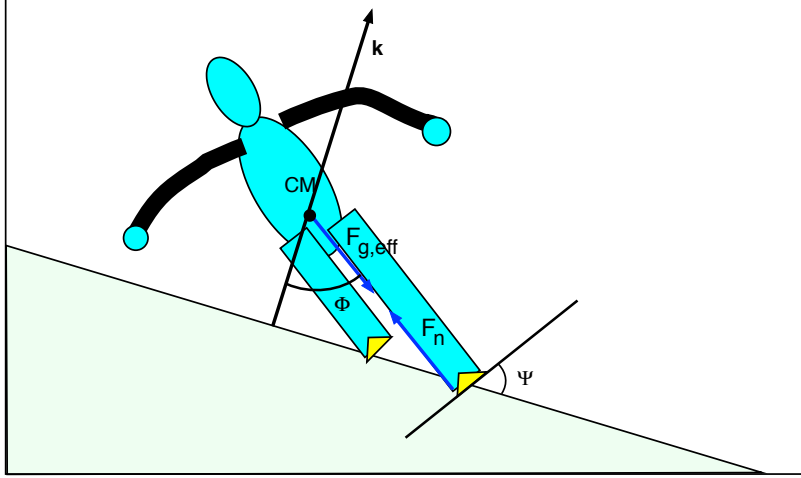
Figure 3. Lateral balance of a stacked (un-angulated) skier. The normal reaction force $\boldsymbol{F}_{\mathrm{n}}$ and the effective gravity force $\boldsymbol{F}_{\mathrm{g,eff}}$ act along the line connecting CM with the inside edge of the outside ski, which results in vanishing torque. The skier inclination angle Φ is the same as the ski edge angle Ψ. This configuration corresponds to the lower-c part of the turn.

smaller value for R_{e}. From the basic geometry of the problem it follows that the effect is significant when the width of the groove platform, on which the ski is resting, becomes comparable to the ski sidecut h_{sc}, which is about 20 mm for a slalom ski. Although his analysis is fine for a stationary ski, the snow plasticity ensures that the ski tail does not return to the surface but instead glides over the platform made in the snow by the forebody of the ski, thus leading to a higher radius than that predicted by the modified Howe equation. Moreover, the finite-element model of the ski-snow interaction by M. Federolf, Lüthi, Roos, and Dual (2010) predicted the turn radius which for $\Psi > 50°$ was even larger than that given by Howe's formula with zero penetration. They speculated that this was due to the higher local sidecut radius of the ski afterbody. To the contrary, in the field study of turns performed by members of the Norwegian national team, Reid, Haugen, Gilgien, Kipp, and Smith (2020) found a good agreement with equation (33) up to $\Psi \simeq 70°$.

A differential twisting (torsion) of the ski about its longitudinal axis, leading to lower value of Ψ at its tip and tail compared to the mid-ski position, increases R_{e}. However, this effect is likely to be marginal. Yoneyama, Scott, Kagawa, and Osada (2008) measured the deflection angle at the ski tip during a ski run to be $\delta\Psi \leq 2°$ and concluded that it had little effect on the geometry of the running edge. Indeed, the effective sidecut of the edge is reduced by $\delta h \simeq d(1 - \cos\delta\Psi)$, where d is the half-width of the ski at the tip. Even for $\delta\Psi$ as high as $10°$ and $d = 60\,\mathrm{mm}$ this leads to $\delta h \approx 0.9\,\mathrm{mm}$.

₃₁₂   Obviously, the applicability of Howe's formula (33) has to be clarified. In our
₃₁₃ study we adopt it, keeping in mind that it may be sufficiently accurate only for icy
₃₁₄ snow.

₃₁₅   The ski trajectory is not the same as the CM trajectory. It is longer and
₃₁₆ in general has higher curvature (e.g. LeMaster, 2010), and so $R > R_{\mathrm{e}}$. This is
₃₁₇ particularly pronounced in short slalom turns (e.g. Reid, 2010; Supej et al., 2014).
₃₁₈ However, the separation between the trajectories is limited by the length of skier
₃₁₉ leg and for sufficiently wide turns we may assume that $R \approx R_{\mathrm{e}}$. Hence, combining
₃₂₀ equations (33) and (25) with the balance condition $\Phi = \Psi$, we find

$$\left(\left(\frac{R_{\mathrm{sc}}}{R}\right)^2 - 1\right)^{1/2} = \frac{v^2}{gR}\frac{1}{\cos\alpha} - \tan\alpha\cos\beta \,. \tag{34}$$

₃₂₁ This is a different form of equation (10-1) in Howe (1983) and it is called by Jentschura
₃₂₂ and Fahrbach (2004) the Ideal-Carving Equation (ICE). It defines R as a function of
₃₂₃ skier's velocity and therefore allows to close the CM equations of motion.

₃₂₄   According to equation (33), R is a monotonically decreasing function of Ψ. It is
₃₂₅ easy to see that $R \to R_{\mathrm{sc}}$ as $\Psi \to 0$ and hence the turn radius of marginally edged ski
₃₂₆ is about R_{sc}. At the other end of the range, $R \to 0$ as $\Psi \to 90°$, which does not make
₃₂₇ much sense and reflects the approximate nature of (33). Obviously, there is a limit
₃₂₈ to how much a ski can be bent before it breaks. If $r_{\mathrm{b}} = R/l_{\mathrm{ski}}$ is the radius of ski
₃₂₉ curvature at the breaking point measured in ski lengths, then we have the constraint
₃₃₀ $\cos\Phi > r_{\mathrm{b}}(l_{\mathrm{ski}}/R_{\mathrm{sc}})$. For a slalom ski with $l_{\mathrm{ski}} = 1.65\,\mathrm{m}$ and $R_{\mathrm{sc}} = 13\,\mathrm{m}$ and the
₃₃₁ fairly reasonable $r_{\mathrm{b}} = 2$, this yields the condition on the ski edge angle $\Psi < 75°$.

₃₃₂   Another upper limit is set by the g-force which builds up during the turn.
₃₃₃ According to LeMaster (2010) the best athletes can sustain the g-force up to about
₃₃₄ three. According to equation (31), this leads to the condition $\Phi < 70°$ (for the realistic
₃₃₅ slope gradient angle $\alpha = 15°$).

₃₃₆   Finally, as Φ increases so does the tangential to the slope component of the
₃₃₇ effective gravity. This is effectively a shearing force acting on the snow. Above a
₃₃₈ certain level it will cause snow fracturing, loss of grip and skidding (Mössner et al.,
₃₃₉ 2009; Mössner et al., 2013). The snow shear stress S relates to $F_{\mathrm{n,c}}$ via

$$F_{\mathrm{n,c}} = l_{\mathrm{ski}}eS \,, \tag{35}$$

₃₄₀ where e is the snow penetration depth in the direction normal to the slope. The
₃₄₁ snow fractures when the shear stress exceeds the critical value S_{c}. Based on equation
₃₄₂ (35) alone one might naively expect that S_{c} sets a lower limit on the snow penetra-
₃₄₃ tion. However, this ignores the fact that the penetration is dictated by the normal
₃₄₄ component $F_{\mathrm{n,k}}$ of the same force. These are related via

$$F_{\mathrm{n,k}} = HV \,, \tag{36}$$

where $V = l_{\mathrm{ski}} e^2/2 \tan \Psi$ is the volume of the imprint made by the ski in the snow and H is the hardness parameter of the snow (Mössner et al., 2013). Combining equations (35,36,32) one finds

$$e < \frac{2S_{\mathrm{c}}}{H}\,, \tag{37}$$

which is an upper limit on the penetration, contrary to the naive expectation. This can be turned into the condition on the skier inclination angle. Indeed, using equations (22,32,36) one finds

$$e^2 = \frac{2mg \cos \alpha \tan \Phi}{H l_{\mathrm{ski}}}$$

and, upon the substitution of this result into equation (37), the condition

$$\tan \Phi < \frac{2S_{\mathrm{c}}^2 l_{\mathrm{ski}}}{mgH \cos \alpha}\,. \tag{38}$$

According to the analysis in Mössner et al. (2013), a well-prepared race track can be attributed with $S_{\mathrm{cr}} \approx 0.52\,\mathrm{N\,mm^{-2}}$ and $H \approx 0.21\,\mathrm{N\,mm^{-3}}$. Using these values along with $m = 70\,\mathrm{kg}$, $l_{\mathrm{ski}} = 165\,\mathrm{cm}$ and $\alpha = 15^o$ we obtain $e < 5\,\mathrm{mm}$ and $\Phi < 81°$. Thus, all three conditions yield approximately the same upper limit on Φ.

Looser snow will fracture under much lower shear stress, thus allowing only small-inclination carving. For example, in their sophisticated multi-body simulations, which incorporated a multi-segment ski model, Mössner et al. (2008) used $H = 0.01\,\mathrm{N\,mm^{-3}}$ and $S_{\mathrm{cr}} = 0.03\,\mathrm{N\,mm^{-2}}$ and observed a transition to skidding during the very first turn. As the turn progressed, the inclination angle of effective gravity increased from $\Phi = 0°$ to $\Phi \approx 45°$. For these snow parameters, $l_{\mathrm{ski}} = 165\,\mathrm{cm}$ and $m = 72\,\mathrm{kg}$, used in their simulations, equation (38) yields the critical angle $\Phi_{\mathrm{c}} = 24°$, which is consistent with the simulation results.

Speed limits imposed by the Ideal Carving Equation

Equation (34) can be written as

$$\left(\xi^2 - 1\right)^{1/2} = a\xi + b\,, \tag{39}$$

where $\xi = R_{\mathrm{sc}}/R$, $a = v^2/gR_{\mathrm{sc}} \cos \alpha$ and $b = -\cos \beta \tan \alpha$. From the definitions it follows that $\xi \geq 1$, $a > 0$ and $|b| < \tan \alpha$. The right-hand side of (39) is the linear function $g(\xi) \equiv \tan \Psi(\xi) = a\xi + b$ which monotonically increases with ξ. The left-hand side of (39) is the radical function $f(\xi) \equiv \tan \Phi(\xi) = \sqrt{\xi^2 - 1}$ which also monotonically increases with ξ. Moreover, since $f'' = -1/\sqrt{\xi^2 - 1} < 0$, f' decreases monotonically from $+\infty$ at $\xi = 1$ to 1 as $\xi \to +\infty$.

Whether the solutions to (39) exist or not critically depends on whether $a < 1$ or $a > 1$. The critical value $a = 1$ corresponds to $v = V_{\mathrm{sc}}$ where

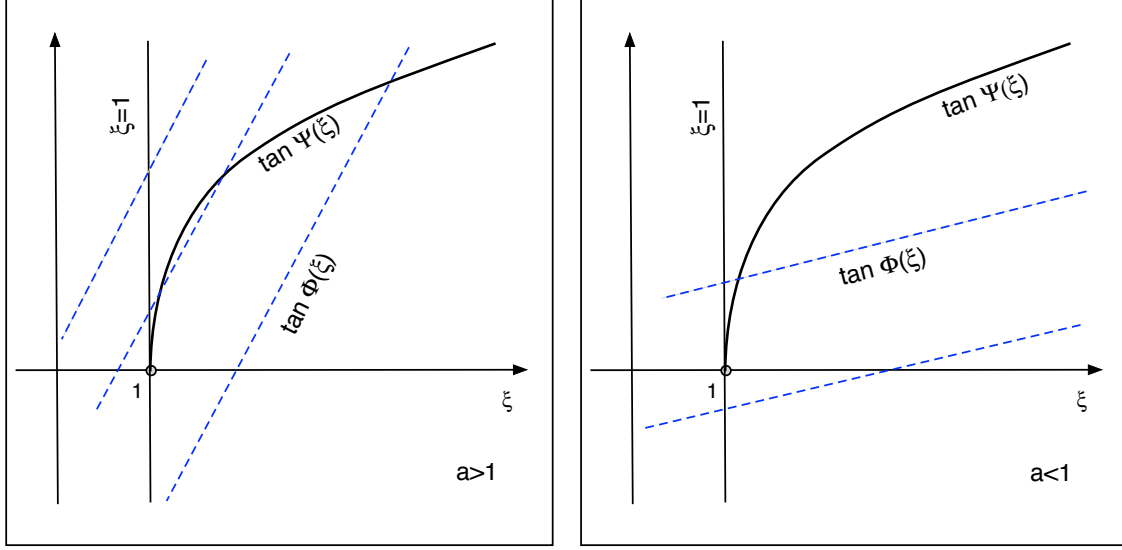$$V_{\mathrm{sc}} = \sqrt{gR_{\mathrm{sc}} \cos \alpha} \tag{40}$$

Figure 4. Finding roots of the ideal carving equation (ICE). The solid line shows $\tan \Psi(\xi) = \sqrt{\xi^2 - 1}$ and the dashed lines $\tan \Phi(\xi) = a\xi + b$. The roots of ICE are given by the intersection points of the curves. *Left panel*: The case $a > 1$. Depending on the value of b, one can have none, one or two roots. *Right panel*: The case $0 < a < 1$. Now one can have either one root or none.

371 (cf. Jentschura & Fahrbach, 2004).

372   When $a < 1$ ($v < V_{\mathrm{sc}}$), the gradient of $g(\xi)$ is lower than the asymptotic gradient
373 of $f(\xi)$ and as illustrated in the right panel of figure 4 there is either one solution
374 or none. The solution exists when $a + b \geq 0$, which includes the case of $b > 0$ and
375 hence there is always a unique solution for the lower-c part of the turn. This solution
376 disappears when $a + b < 0$ which implies negative b and hence the upper-c part of
377 the turn. In terms of the turn speed and the angle between the skier velocity and the
378 fall line, $\gamma = |\beta - 90°|$, the existence condition reads

$$\sin \gamma \leq \frac{v^2}{gR_{\mathrm{sc}} \sin \alpha}. \tag{41}$$

Thus, for sufficiently low speeds, namely $v^2 < gR_{\mathrm{sc}} \sin \alpha$, carving is possible only close
to the fall line. In order to understand this result, consider a stationary skier whose
skis point perpendicular to the fall line. In order to stay in balance the skier has to be
aligned with the vertical direction and this implies ski edging which is consistent with
the lower-c part of the turn only. Hence, if the skier is pushed forward just a little bit
then their trajectory will turn not downhill but uphill. To turn downhill the skis must
be at least flat on the snow (or marginally edged) in which case they carve an arc of
the radius $R = R_{\mathrm{sc}}$. The balance condition (26) then implies that the corresponding
centrifugal force mv^2/R_{sc} must be high enough to balance the centripetal component

of the gravity force $mg \sin \alpha \cos \beta$. This yields the speed

$$v^2 = gR_{\mathrm{sc}} \sin \alpha \sin \gamma \,,$$

379 in agreement with condition (41).

When $a > 1$ ($v > V_{\mathrm{sc}}$), the gradient of $g(\xi)$ is higher than the asymptotic gradient of $f(\xi)$ and as one can see in the left panel of figure 4 there are three distinct possibilities. If $g(1) = a + b < 0$ then there exists one and only one root. As we increase b above $-a$, then initially there are two roots but eventually they merge and disappear. The bifurcation occurs at the point ξ_{c} where

$$g(\xi_{\mathrm{c}}) = f(\xi_{\mathrm{c}}) \quad \text{and} \quad g'(\xi_{\mathrm{c}}) = f'\xi_{\mathrm{c}} \,.$$

380 Solving these two simultaneous equations for ξ_{c} and b_{c}, we find that

$$b_{\mathrm{c}} = -(a^2 - 1)^{1/2} \quad \text{and} \quad \xi_{\mathrm{c}} = \frac{a}{(a^2 - 1)^{1/2}} \,. \tag{42}$$

381 There are no solutions when $b > b_{\mathrm{c}}$, which includes all positive values of b and hence
382 the whole lower-c part of the turn. This means that at such high speeds balanced
383 carving turns are impossible.

What are the indications that a skier is about to hit the speed limit V_{sc}? Consider the entrance point to the lower-c part of the turn. At this point $\beta = 90°$, $b = 0$ and hence equation (39) reads

$$\left(\xi^2 - 1\right)^{1/2} = a\xi \,.$$

Its solution

$$\xi = \frac{1}{\sqrt{1 - a^2}} \to \infty \quad \text{as} \quad a \to 1 \,.$$

Thus the turn becomes very tight (formally $R \to 0$) and the skier's body close to horizontal (formally $\Phi \to 90°$). On approach to this point something will give up. As we discussed earlier this will be either the skis, the skier's legs or the snow resistance to the applied shearing force. If however the speed limit is exceeded in the upper-c part of the turn, there may not be such a clear indicator. In fact, after this the turn can be continued for a while until it reaches the critical traverse angle β_{c} where

$$\cos \beta_{\mathrm{c}} = \cot \alpha \left(\left(\frac{v}{V_{\mathrm{sc}}} \right)^4 - 1 \right)^{1/2}$$

384 and

$$\tan \Phi_{\mathrm{c}} = \left(\left(\frac{v}{V_{\mathrm{sc}}} \right)^4 - 1 \right)^{-1/2} \tag{43}$$

385 (see equations 42). When v grows slowly at the point of going over V_{sc}, the loss
386 of balance occurs close to the fall line at extreme inclination angles. If however the

387 growth is fast, v may significantly overshoot $V_{\rm sc}$ quite early in the upper-c part of
388 turn. In this case the loss of balance may also occur early and at Φ significantly below
389 $90°$.

390   Figure 4 shows that when $v > V_{\rm sc}$ no balanced position exists because for any
391 turn radius $\Phi > \Psi$. The effective gravity is not directed along the lever arm but
392 points away from it, resulting in non-vanishing net torque about the point where the
393 carving ski is "pinned" to the snow. This torque pushes the skier body away from
394 the slope towards the position with zero inclination.

395   It is easy to show that

$$V_{\rm sc} = V_{\rm g} \left(\frac{R_{\rm sc}}{L_{\rm g} \tan \alpha} \right)^{1/2} . \tag{44}$$

396 For the typical parameters of slalom competitions, this gives

$$V_{\rm sc} = 0.3 V_{\rm g} \left(\frac{R_{\rm sc}}{13\,{\rm m}} \right)^{1/2} \left(\frac{L_{\rm g}}{200\,{\rm m}} \right)^{-1/2} \left(\frac{\tan \alpha}{\tan 20°} \right)^{-1/2} . \tag{45}$$

397 Thus, for carving turns in slalom $V_{\rm sc}$ is significantly smaller than the characteristic
398 speed $V_{\rm g}$ (see equation 8) set by the aerodynamic drag. This suggests that pure carv-
399 ing turns are normally impossible for the typical parameters of slalom competitions
400 and the racers have to shave their speed via skidding on a regular basis. The only
401 exceptions are probably (i) low gradient sections of the track where the last factor
402 of equation (45) can be sufficiently large, (ii) the first few turns right after the start,
403 where the speed has not yet approached $V_{\rm sc}$ and (iii) the few turns at the transitions
404 from steep to flat part of the race track. In the last case, $V_{\rm sc}$ significantly increases
405 at the transition, giving to the racer the opportunity to increase their speed as well.
406 It is easy to verify that the situation is quite similar in other race disciplines.

Stability

408   The equilibrium of a stacked skier who keeps all the load on the outside ski
409 is similar to that of an inverted pendulum and hence unstable (Lind and Sanders
410 (1996), Appendix B). However, skiers have ways of controlling this instability. Lind
411 and Sanders (1996) discuss the stabilising arm moment, similar to what is used by
412 trapeze artists. Ski poles can provide additional points of support when planted into
413 or dragged against the snow. Some control can be provided by the body angulation
414 (Appendix B). Finally and presumably most importantly, when both skis are suffi-
415 ciently wide apart and loaded, instead of the unique balanced inclination angle we
416 have a continuum of balanced positions (see Appendix B) and so small perturbations
417 just shift the skier to nearby equilibria. Moreover, this gives to skiers a simple way
418 of controlling their inclination angle – via relaxing and extending their legs.

419 Dimensionless equations of carving turn

It is common practice of mathematical modelling to operate with dimensionless equations, which are derived using a set of scales characteristic to the problem under consideration, instead of standard units. This leads to simpler equations which are easier to interpret and to the results which are at least partly scale-independent. Since in ideal balanced carving the speed must stay below V_{sc} this is a natural speed scale. Because the turn radius is limited by R_{sc} this is a convenient length scale. The corresponding time scale is $T_{\mathrm{sc}} = R_{\mathrm{sc}}/V_{\mathrm{sc}}$. In order to derive the dimensionless equations of balanced carving we now write

$$v = V_{\mathrm{sc}}\tilde{v}\,, \quad t = T_{\mathrm{sc}}\tilde{t}\,, \quad R = L_{\mathrm{sc}}\tilde{R}\,,$$

420 substitute these into the dimensional equations and where possible remove common
421 dimensional factors. Finally, we ignore tilde in the notation. In other words, we do
422 the substitutions $v \to V_{\mathrm{sc}}v$, $t \to T_{\mathrm{sc}}t$, $R \to R_{\mathrm{sc}}R$ and then simplify the results. For
423 example, the substitution $v \to V_{\mathrm{sc}}v$ into the equation (7) gives the dimensionless
424 equation for the saturation speed of fall-line gliding

$$v_{\mathrm{S}} = \mathrm{Sr}\sqrt{1 - \mu \cot \alpha}\,, \tag{46}$$

425 which includes the dimensionless speed parameter $\mathrm{Sr} = V_{\mathrm{g}}/V_{\mathrm{sc}}$. Similarly, we deal
426 with other dimensional variables should they appear in the equations, e.g. $x \to R_{\mathrm{sc}}x$
427 and $y \to R_{\mathrm{sc}}y$. In particular, the application of this procedure to (20) gives the
428 dimensionless speed equation

$$\frac{dv}{dt} = \sin \beta \tan \alpha - \frac{\mu}{R} - \mathrm{K}v^2\,, \tag{47}$$

429 where

$$\mathrm{K} = \frac{R_{\mathrm{sc}}}{L_{\mathrm{g}}}\,, \tag{48}$$

430 is a dimensionless parameter which we will call the dynamic sidecut parameter. The
431 g-force can be written as

$$\text{g-force} = \frac{\cos \alpha}{R}\,. \tag{49}$$

432 The dimensionless ideal-carving equation (34) reads

$$\left(\frac{1}{R^2} - 1\right)^{1/2} = \frac{v^2}{R} - \cos \beta \tan \alpha\,. \tag{50}$$

433 The equation governing the evolution of β follows from equation (18) upon the sub-
434 stitution $dl = v\,dt$. It reads

$$\frac{d\beta}{dt} = \frac{v}{R} \tag{51}$$

and the dimensionless skier coordinates can be found via integrating

$$\frac{dx}{dt} = \mp v \cos \beta \,, \tag{52}$$

where we use the sign minus for right turns and the sign plus for left turns, and

$$\frac{dy}{dt} = v \sin \beta \,. \tag{53}$$

Equations (47-53) determine the arc of a carving turn and the skier motion along the arc. What they do not tell us is when one turn ends and the next one begins. These transitions have to be introduced independently. In this regard the angle of traverse is a more suitable independent variable than the time because its value is a better indicator of how far the turn has progressed. Replacing t with β via equation (51) we finally obtain the complete system of equations which we use to simulate carving runs in this study. It includes three ordinary differential equations

$$\frac{dv}{d\beta} = \frac{R}{v} \left(\sin \beta \tan \alpha - \frac{\mu}{R} - \mathrm{K} v^2 \right) \,, \tag{54}$$

$$\frac{dx}{d\beta} = \mp R \cos \beta \,, \tag{55}$$

$$\frac{dy}{d\beta} = R \sin \beta \,, \tag{56}$$

and the constitutive equation

$$\left(\frac{1}{R^2} - 1 \right)^{1/2} = \frac{v^2}{R} - \cos \beta \tan \alpha \,. \tag{57}$$

The definition of β implies that it increases both during the left and the right turns, but not in the transition between turns. In our simplified model of the transition, the direction of motion $\boldsymbol{u}$ remains unchanged and hence the angle of traverse has to change from β to $180° - \beta$. According to equation (57) this implies a jump in the local turn radius and hence the skier inclination. As a result, during the whole run, which may consist of many turns, β remains confined between $0°$ and $180°$, provided each turn terminates before going uphill.

Finally, we observe that equations (54) and (57) do not involve x and y and hence can be solved independently from equations (55-56). However, all these equations should be integrated simultaneously when we are interested in a skier's trajectory. Equation (51) should be added as well when we need to know the run evolves in time.

<center>**Results**</center>

Here we present the results of our study of ideal carving runs as described by equations (54-57) with instantaneous transitions between turns. At the start we specify the initial angle of traverse β_{ini} and speed v_{ini}, achieved during the run-up phase. Each turn is terminated when the traverse angle reaches a given value, denoted as β_{fin}. Hence, beginning from the second turn, all turns are initiated at $\beta_{\text{ini}} = 180° - \beta_{\text{fin}}$. Initially we focus on the effect of slope steepness and fix the sidecut parameter to $K = 0.0325$ and the coefficient of friction to $\mu = 0.04$. For the aerodynamic length scale $L_{\text{g}} = 200\,\text{m}$ this corresponds to SL skis with the dimensional radius of $R_{\text{sc}} = 13\,\text{m}$. Later we discuss the effect of sidecut radius as well.

Gentle slope

First we consider a slope with $\alpha = 5°$. For such a gentle ("flat") slope, the speed of fall-line gliding saturates at $v_{\text{s}} = 0.737 V_{\text{g}}$. However, the speed limit $V_{\text{sc}} = 0.612 V_{\text{g}} < v_{\text{s}}$, indicating that the skier speed may eventually exceed V_{sc}.

Here we present the results for the run with $x_{\text{ini}} = y_{\text{ini}} = 0$, $\beta_{\text{ini}} = 0.3\pi$ (54°), $v_{\text{ini}} = 0.49 V_{\text{sc}}$ ($0.3 V_{\text{g}}$) and $\beta_{\text{fin}} = 0.9\pi$ (162°). Figure 5 shows the trajectory of this run, which exhibits a rather slow evolution of the turn shape. This agrees with the data presented in Figure 6, which shows the evolution of R, v, Φ and the g-force for the first 20 turns. Indeed, the turn radius does not vary much along the track. Moreover, although each next turn is not an exact copy of the previous turn, for each of the variables we observe convergence to some limiting curve, which will refer to as the asymptotic turn solution. In practical terms, well down the slope each next turn becomes indistinguishable from the previous one. This is reminiscent of the so-called limit cycle solutions in the theory of dynamical systems.

Interestingly, the speed of the asymptotic solution remains well below v_{s} and even below V_{sc}, with the mean value $\langle v \rangle \approx 0.75 V_{\text{sc}}$. This is due to the higher work done by the friction force compared to the fall-line gliding because of 1) the longer trajectory of this run compared to the straight fall line and 2) the fact that the effective weight of skier is higher than mg, leading to higher friction force. In order to verify this explanation one can use the equilibrium version of the speed equation (54)

$$\langle \sin \beta \rangle \tan \alpha - \mu \langle \frac{1}{R} \rangle - K \langle v^2 \rangle = 0 \,, \tag{58}$$

where $\langle A \rangle$ stands for the mean turn value of the quantity A. According to figure 6, $\langle 1/R \rangle = \langle \text{g-force} \rangle / \cos \alpha \approx 1.2$ whereas $\langle \sin \beta \rangle$ can be estimated via

$$\langle \sin \beta \rangle = \frac{1}{0.8\pi} \int\limits_{0.1\pi}^{0.9\pi} \sin(\beta) d\beta \approx 0.796 \,.$$

Substituting the estimates into equation (58), we find $\langle v \rangle \approx 0.8 V_{\text{sc}}$, which is quite
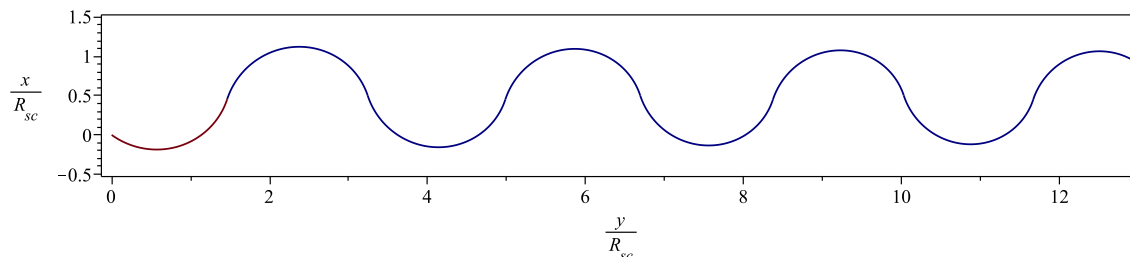
Figure 5. The first few turns of the flat-slope run ($\alpha = 5°$).

close to what we see in the numerical data. For $R_{\mathrm{sc}} = 13\,\mathrm{m}$, the corresponding dimensional value is $\langle v \rangle \approx 27\,\mathrm{km/h}$.

Moderately steep slope

Here we deal with a slope with $\alpha = 15°$. For this slope $v_{\mathrm{s}} = 0.922 V_{\mathrm{g}}$ and $V_{\mathrm{sc}} = 0.35 V_{\mathrm{g}}$ is now significantly below v_{s}. Figure 7 shows the trajectory of the run with the same initial parameters and β_{fin} as in the case of flat slope. On can see that now the turns are much shorter and not so rounded, with the individual turn shape reminiscent of the letter "J", rather than "C" . Figure 8 shows the evolution of R, v, Φ and the g-force for the first 20 turns of this run. Like in the flat-slope case, the solution converges to an asymptotic one but now this occurs very quickly – the individual turn curves become indistinguishable beginning from the forth turn. The top-left panel of figure 8 confirms that on average the turn radius is significantly lower than in the flat run. Moreover, it varies dramatically, from $R \approx 0.6 R_{\mathrm{sc}}$ at the turn initiation down to $R \approx 0.12 R_{\mathrm{sc}}$ soon after the fall-line. The latter is approximately 1.6m (one SL ski length) when the solution is scaled to $R_{\mathrm{sc}} = 13\mathrm{m}$.

Rather surprisingly, the speed of the asymptotic solution still remains below V_{sc}, but only just, and well below V_{g}. The latter shows that contrary to the expectations based on the analysis of fall-line gliding, in this slalom run the aerodynamic drag is not the dominant factor in determining the saturation speed. The reason is the extremely high effective weight and hence the friction force. According to Figure 8, $\langle 1/R \rangle \approx 5$ and $\langle v \rangle \approx 1$. Hence, in equation (58) the geometric term $\langle \sin \beta \rangle \tan \alpha \approx 0.213$, the friction term $\langle \mu/R \rangle \approx 0.2$ and the aerodynamic drag term $\mathrm{K}\langle v^2 \rangle \approx 0.03$. Thus, the geometric and the friction terms almost balance each other, whereas the contribution of the aerodynamic drag is small.

The corresponding dimensional value of the mean skier speed in the asymptotic solution is $v \approx 35$ km/h, which is not that far below the typical speed of slalom competitions. However, the inclination angle of this run reaches very high values, $\Phi \approx 80°$ in the lower-c part of the turn and the g-force is extremely high. This shows

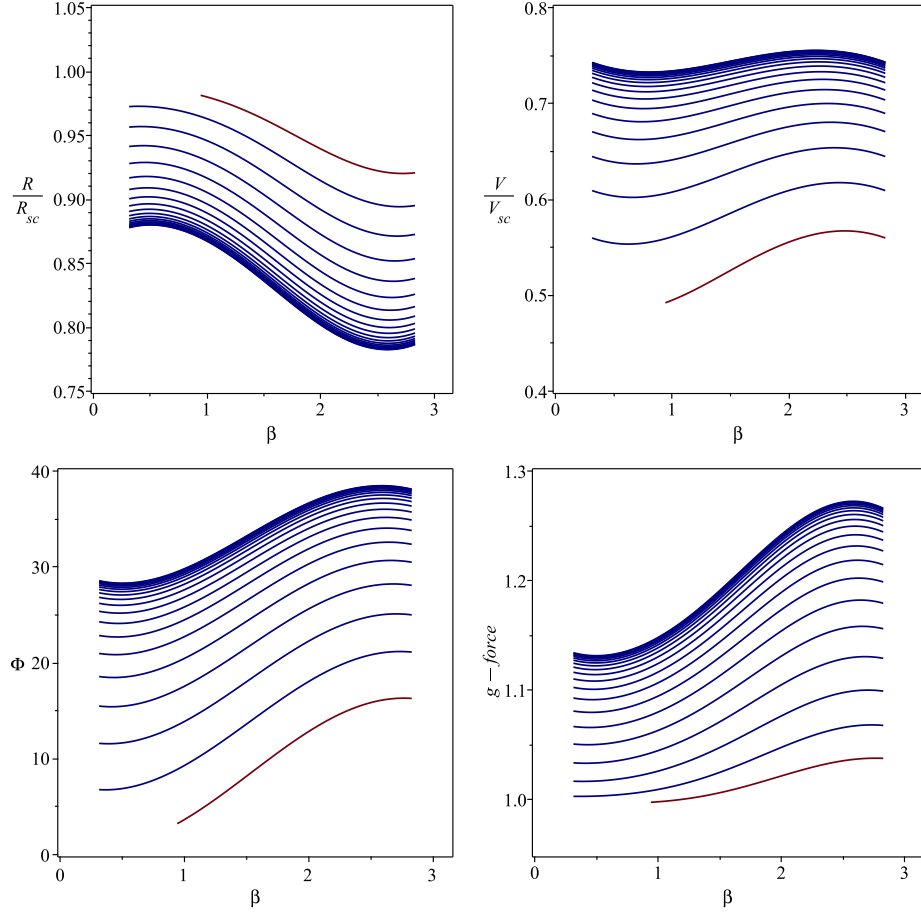*Figure 6*. Evolution of $R(\beta)$, $v(\beta)$, $\Phi(\beta)$ and F_n for the flat-slope run ($\alpha = 5°$) during the first 20 turns. In each of these plots, there are 20 curves which show the evolution of these variables during each turn. Each such curve (except the one corresponding to the first turn which originates at $\beta = 0.3\pi$) originates at $\beta = 0.1\pi$ (the turn initiation point) and terminated at $\beta = 0.9\pi$ (the turn completion point). The transition between turns is a jump from the termination point of the previous turn to the initiation point of the next turn. In the R-panel this transition is a jump to the lower curve and in the v-, Φ- and F_n-panels to the upper curve.
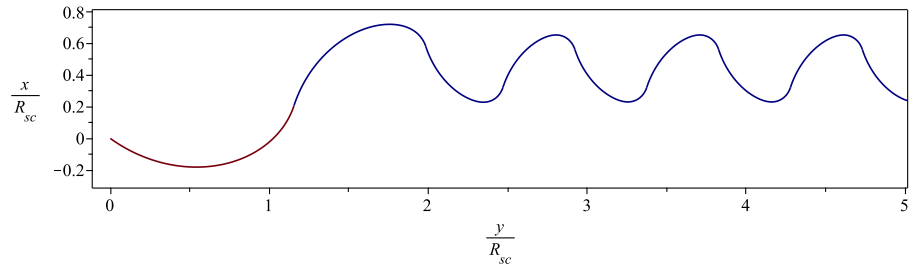
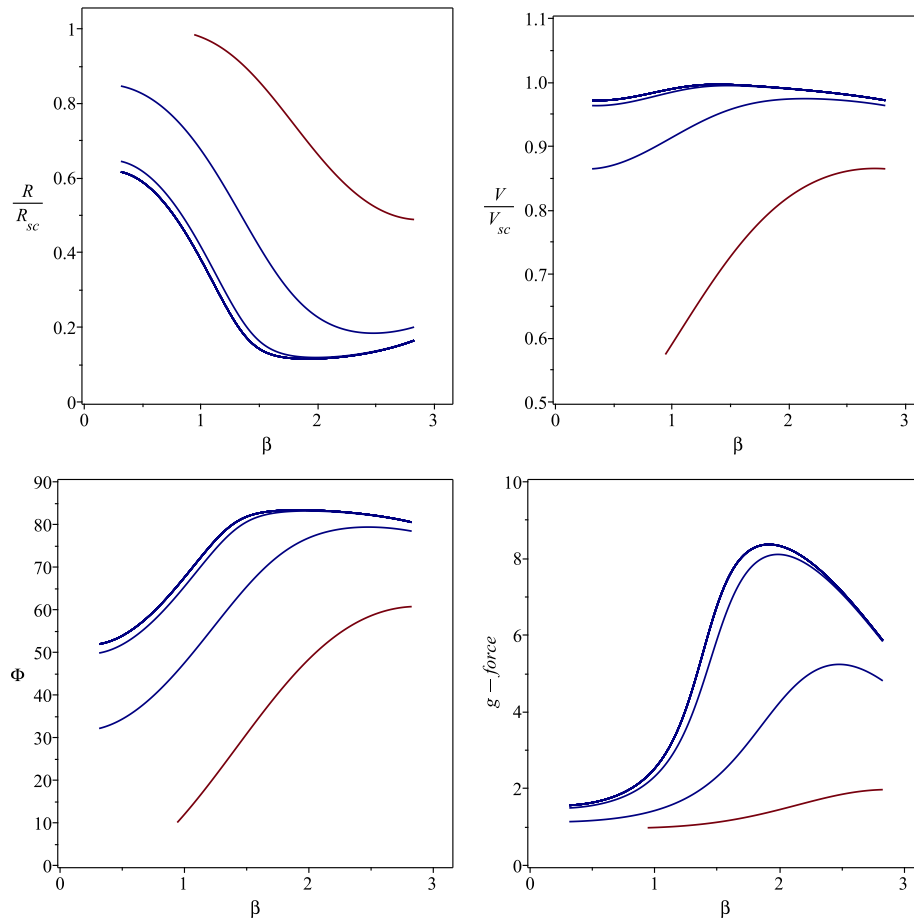*Figure 7*. The first few turns for the moderately steep slope ($\alpha = 15°$).

Figure 8. The same as in figure 6 but for the moderately steep slope ($\alpha = 15°$).

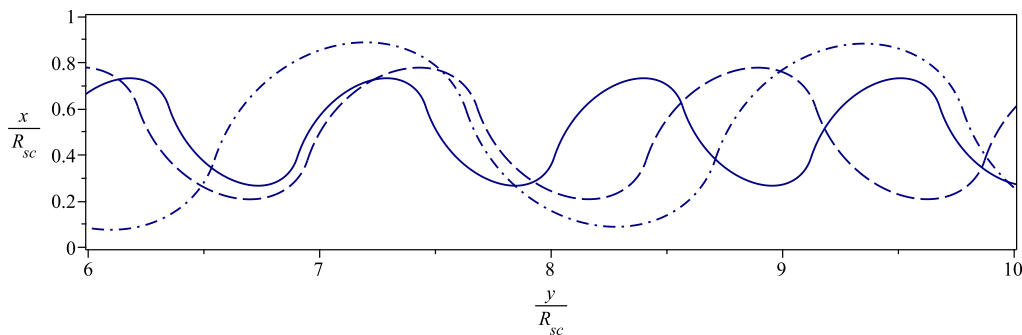*Figure 9.* The trajectories of ideal carving runs on the $\alpha = 13°$ slope with slalom (solid), giant slalom (dashed) and downhill (dash-dotted) skis.

that in this run we are beyond what is achievable in practice.

For a steep slope with $\alpha = 35°$, V_{sc} is reached very quickly and the carving run cannot be continued beyond the first turn.

The approximate similarity of balanced carving runs

How different are the carving turns in different alpine disciplines? The equations of carving turn (54–57) have only three dimensionless parameters that modify these equations and hence their solutions – the coefficient of dynamic friction μ, the slope angle α and the dynamic sidecut parameter $K = R_{\mathrm{sc}}/L_{\mathrm{g}} \ll 1$. If K was negligibly small then the equations would be practically non-dependent on R_{sc}. This means that for the same slope angle and coefficient of friction (the same snow conditions and wax), the slalom and downhill carving runs would be just scale versions of each other, with the trajectory scaling as $\propto R_{\mathrm{sc}}$, skier's speed as $\propto V_{\mathrm{sc}} \propto \sqrt{R_{\mathrm{sc}}}$ and the g-force and inclination angle both remaining unchanged.

Equation (54) tells us that a higher value of K leads to a lower speed in the asymptotic solution. Because of this and the fact that $K \propto R_{\mathrm{sc}}$, the expect v/V_{sc} to be actually a bit smaller for a discipline where skis have larger R_{sc}. If so then equation (57) ensures a larger R/R_{sc}, equation (49) a weaker g-force and equation (33) a smaller inclination angle. To check this, we compared solutions corresponding to SL, GS (giant slalom) and DH skis for $\alpha = 13°$ and $\mu = 0.04$. Figure 9 shows the dimensionless trajectories of these runs in the asymptotic regime. Although they are relatively similar they are still not exact copies of one another, with larger K yielding longer and smoother turns as expected. Figure 10 shows the behaviour of other parameters which also agrees with our expectations.

In the speed equation (54), K is the coefficient of the aerodynamic drag term Kv^2. Hence, we the deviation from the simple scaling found in the case $K = 0$ reflects

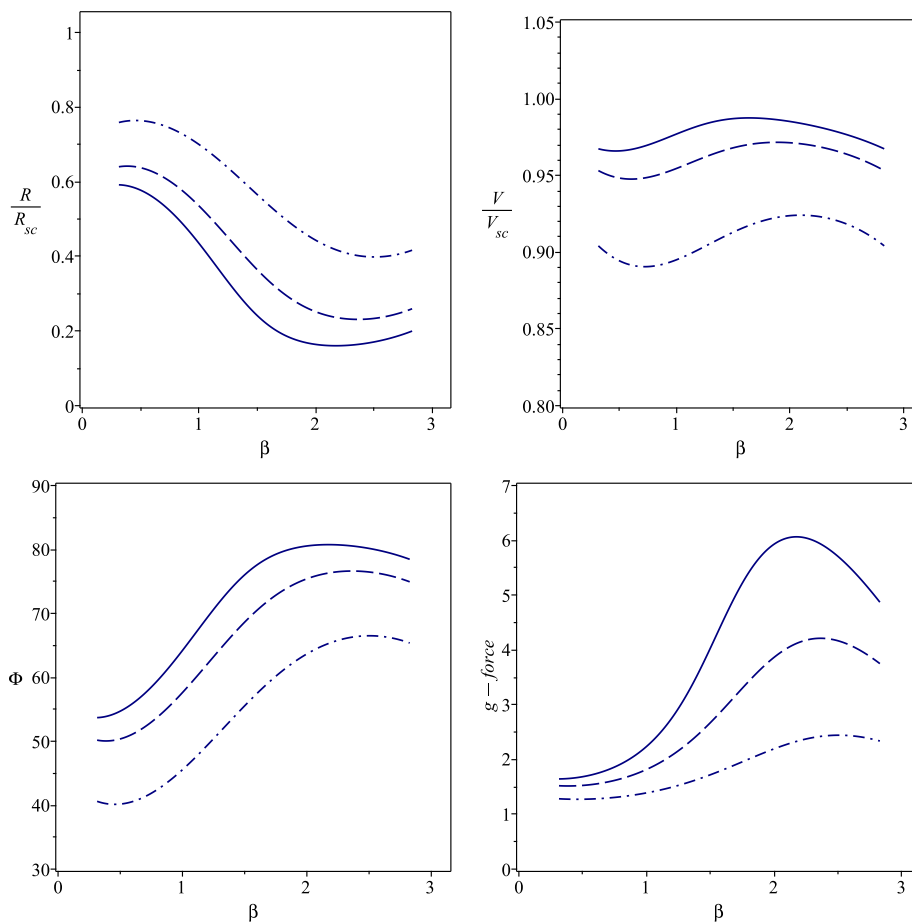*Figure 10.* The asymptotic turn parameters for ideal carving runs on the $\alpha = 13°$ slope with slalom (solid), giant slalom (dashed) and downhill (dash-dotted) skis.

543 the variation in the relative importance of the aerodynamic drag. Its role increases
544 as we move from SL towards DH, which is a well-known fact.

545 **The snow friction and the critical slope gradient**

546   We extended the study described in the previous sections in order to determine
547 the critical slope steepness $\alpha_{c,t}$ above which pure balanced carving is impossible for
548 SL, GS and DH skis even theoretically (v exceeds V_{sc}). The result is

$$\alpha_{c,t} = \begin{cases} 17° & \text{for} \quad K = 0.0325\,(13\text{m})\,, \\ 19° & \text{for} \quad K = 0.0875\,(30\text{m})\,, \\ 21° & \text{for} \quad K = 0.1250\,(50\text{m})\,, \end{cases} \tag{59}$$

549 where in the brackets we show the dimensional sidecut radius corresponding to $L_g =$
550 200m. Here we also observe only a relatively weak dependence on R_{sc}. When the

limitations based on the shear resistance of snow, physical strength of skiers and structural strength of skis are taken into account, the practical critical gradients become even smaller.

The result (59) was obtained for the friction coefficient $\mu = 0.04$. However, the coefficient depends on many factors and may vary significantly. Since a higher friction coefficient μ implies a lower saturation speed of the run and hence a weaker centrifugal force, this may also allow carving on steeper slopes. We explored this avenue using a little more pragmatic definition of executable carving turns. Namely, we demanded that the inclination angle Φ did not exceed $\Phi_c = 70°$.

We run SL and DH models with μ=0.04, 0.07 and 0.10. For each model we used a simple iterative procedure aimed at identifying the slope angle for which in the asymptotic solution Φ peaked within one percent of Φ_c. The results are shown in figure 11. They are well fitted by the linear equations

$$\tan \alpha_c = 2.3\mu + 0.06 \,. \tag{60}$$

for the SL skis (K = 0.0325) and

$$\tan \alpha_c = 2.2\mu + 0.16 \,. \tag{61}$$

for the DH skis (K = 0.125).

The effect of angulation

So far we limited our analysis to the case of stacked skier where the skier inclination to the slope (the lever-arm inclination) is the same as the edge angle of their skis. However, skiers often angulate their body by moving hip and to some degree knees towards the inside of the turn. In this case, CM shifts from the belly button towards the outside of the turn and hence the edge angle becomes higher than the lever-arm inclination (see figure 12). As the torque balance still requires the inclination of the effective gravity force to be the same as the lever arm inclination, this leads to $\Theta = \Psi - \Phi > 0$.

There are at least two benefits of such angulation. Firstly, it is known to introduce a better safety margin against accidental side-slipping of the skis (skidding). Secondly, it allows to vary the turn radius, thus introducing some control over the carving turn (e.g. Harb, 2006; Howe, 1983).

We note here that when $\Theta > 0$ the ski is pressed not only against the base of the platform it creates in the snow but also against the wall of this platform (see figure 12). Hence, the total normal reaction force of the snow $\boldsymbol{F}_n = \boldsymbol{F}_{n,b} + \boldsymbol{F}_{n,w}$ is the sum of the force $\boldsymbol{F}_{n,b}$ originated from the base and the force $\boldsymbol{F}_{n,w}$ originated from the wall and because of this it may still be aligned with the effective gravity force.

Using the notation introduced in our analysis of ICE, $\tan \Psi = (\xi^2 - 1)^{1/2}$ and $\tan \Phi = a\xi + b$. For $0 < \Phi < \Psi < 90°$, we can write $\tan \Psi = \eta \tan \Phi$ where $\eta > 1$,
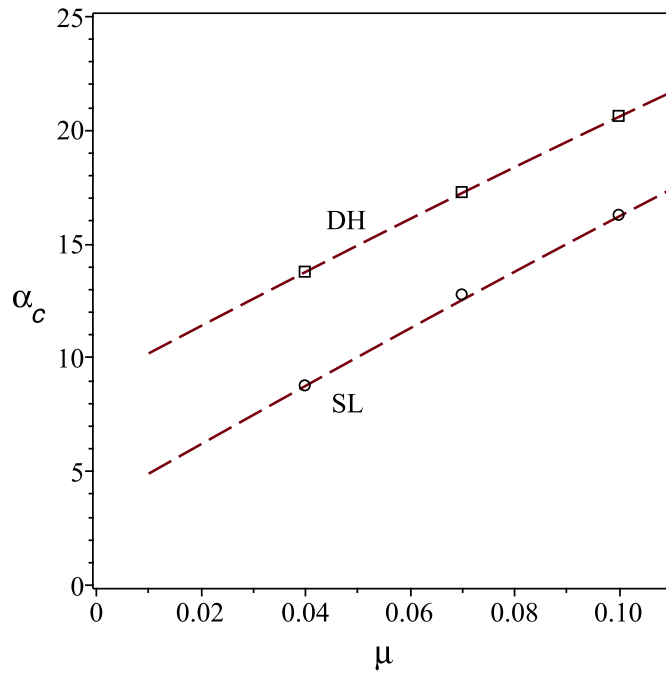
Figure 11. The critical slope gradient as a function of the friction coefficient for $\Phi_c = 70°$. The markers show the numerical data and the dashed lines their fit by the linear functions (60,61).
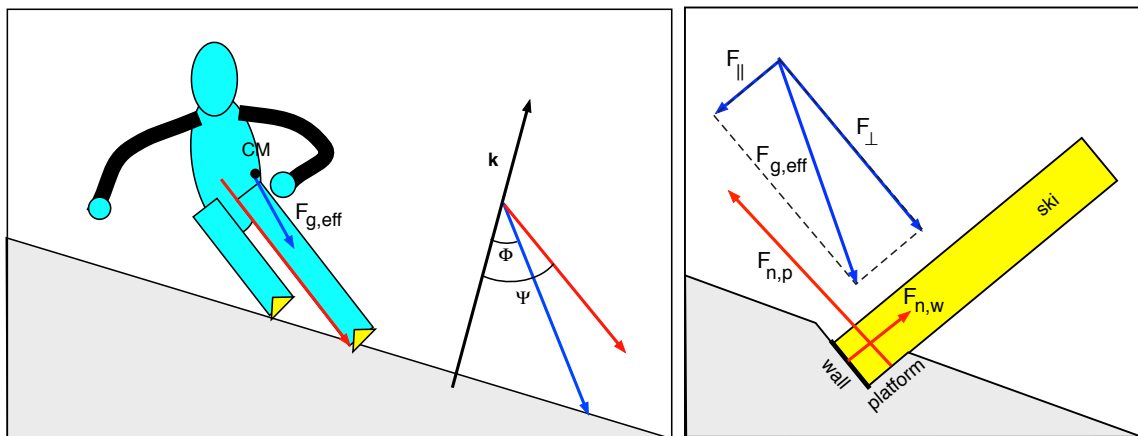

Figure 12. Inclination and angulation. Left panel: Because of the angulation at the hip, the ski edge angle Ψ is higher than the inclination angle of the skier Φ. Right panel: Because $\Psi > \Phi$ the effective gravity has not only the component normal to the platform cut in the snow by the ski ($\boldsymbol{F}_\perp$) but also the component parallel to the platform and pushing the ski into the platform wall ($\boldsymbol{F}_\parallel$). The wall reacts with the force $\boldsymbol{F}_{n,w}$, balancing $\boldsymbol{F}_\parallel$.
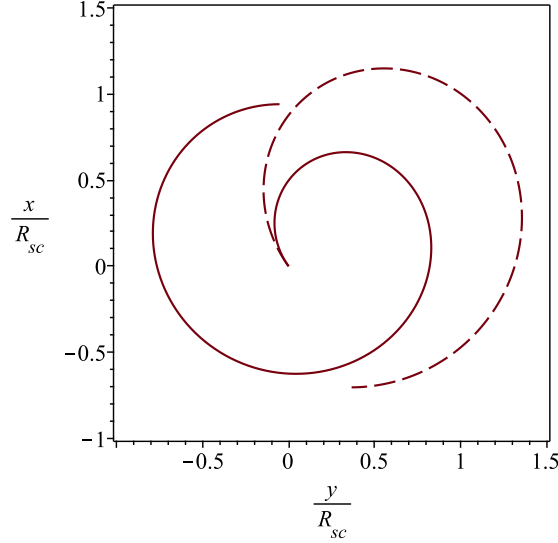
Figure 13. Trajectories of attempted 360° carving turns with (solid line) and without (dashed line) angulation. The trajectory of the turn without angulation terminates at the point where the skier comes to halt, whereas the trajectory of the turn with angulation is terminated arbitrary and the skier speed at the termination point does not vanish.

which yields the modified ideal carving equation

$$(\xi^2 - 1)^{1/2} = \eta(a\xi + b) \,. \tag{62}$$

Introducing $a' = \eta a > a$ and $b' = \eta b > b$, we can write equation (62) in exactly the same form as the original ICE (Eq.34) but with the primed parameters in the place of the original unprimed ones. This immediately allows us to deduce the effect of the angulation on the speed limits of balanced carving. Since $a + b > 0$ if and only if $a' + b' > 0$, the lower speed limit (41) remains unchanged. However, the condition $a' < 1$ now yields the constraint

$$v < V_{\mathrm{sc}}(\eta) \quad \text{where} \quad V_{\mathrm{sc}}(\eta) = \sqrt{\frac{gR_{\mathrm{sc}}}{\eta} \cos\alpha} \,. \tag{63}$$

Thus, the upper speed limit is reduced.

In order to elucidate the effect of angulation further, we analysed the so-called 360°-carving turn. By this we understand a carving turn which continues in the clockwise (or counter-clockwise) direction all the way – first downhill, then uphill and finally downhill again without any interruption. In this example, we assumed that the skier angulation depended only on the inclination angle, $\Theta = \Theta(\Phi)$, as described by the equation
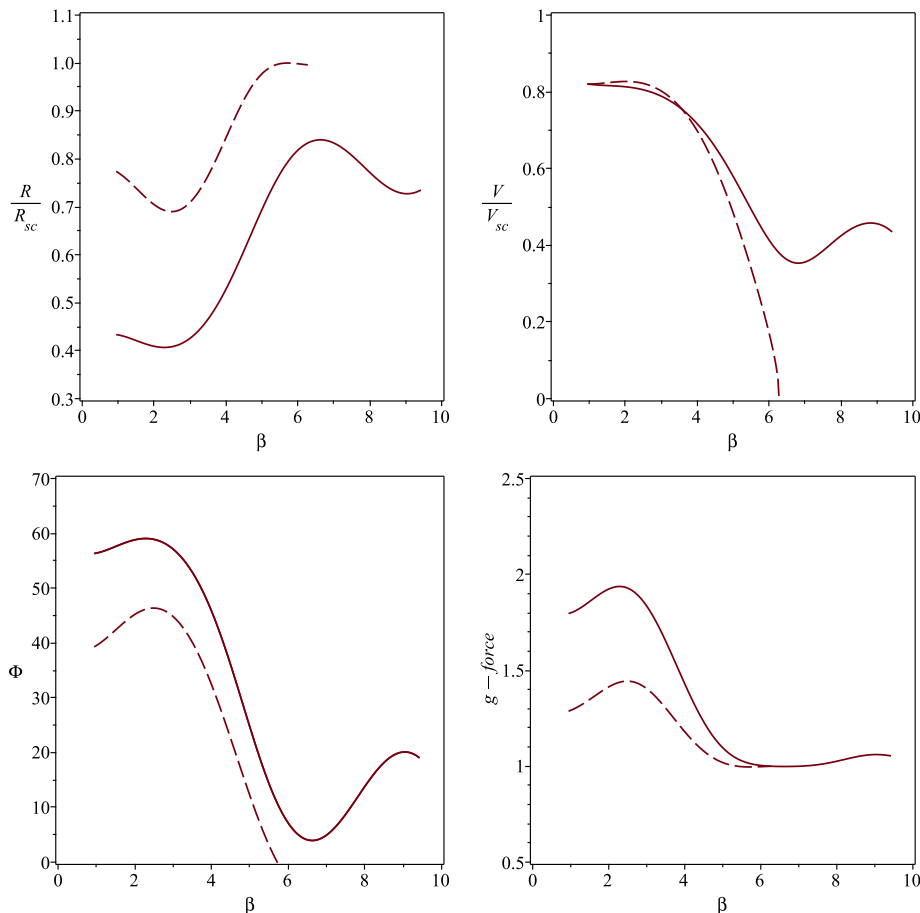
$$\tan\Psi = A + \tan\Phi \,, \tag{64}$$

Figure 14. The attempts at 360° turn with (solid lines) and without (dashed lines) angulation.

where A is constant. It is easy to see that $A = \tan(\Theta(0))$. It is also easy to verify that $\Theta(\Phi)$ is a monotonically decreasing function which vanishes as $\Phi \to 90°$, and that it yields $\Psi < 90°$ for all $0 \leq \Phi < 90°$.

Here we present the results for the slope angle $\alpha = 5°$, the initial skier speed $v_{\text{ini}} = 0.5 V_{\text{g}}$ and the initial angle of traverse $\beta_{\text{ini}} = 54°$. Such a high speed could be gained at a preceding steeper uphill section of the slope. Figures 13 and 14 show the results for two runs: one with no angulation ($A = 0$, dashed lines) and one with strong angulation ($A = \tan(30°)$, solid lines). The run without angulation fells a bit short of success. It stops on approach to the summit as the skier's speed drops to zero. In the run with angulation, the turn is much tighter and the skier reaches the summit retaining a fair fraction of the initial speed. This allows them to continue and complete the 360°-turn. Because of the similar initial speed but the lower turn radius, the centrifugal force, and hence the total g-force of this run, is higher, making the turn physically more demanding. Moreover, the skier skeleton is no longer well

stacked and hence bears a smaller fraction of the total skier's weight. This spells an increased risk of injury.

The effect of loading the inside ski

In our study here, we focused on the case where the skier balances entirely on the inner edge of the ski which is located on the outside of the turn's arc. Indeed, one of the first things learned in ski lessons is keeping most of the load on the outside ski. However, some loading of the inside ski is needed to gain in stability, turn control and reduction of stress on the outside leg.

Let us briefly analyse the effect of partial loading of the inside ski in carving turns. Denote as $\boldsymbol{F}_{\mathrm{n,i}}$ and $\boldsymbol{F}_{\mathrm{n,o}}$ the normal reaction forces from the inside and the outside skis, respectively, and as $\boldsymbol{r}_{\mathrm{i}}$ and $\boldsymbol{r}_{\mathrm{o}}$ the position vectors connecting the skier's CM with the inner edges of the skis in the transverse plane. The force balance then reads

$$\boldsymbol{F}_{\mathrm{g,eff}} + \boldsymbol{F}_{\mathrm{n,i}} + \boldsymbol{F}_{\mathrm{n,o}} = 0 \,, \tag{65}$$

whereas the torque balance in the transverse plane is

$$\boldsymbol{r}_{\mathrm{i}} \times \boldsymbol{F}_{\mathrm{n,i}} + \boldsymbol{r}_{\mathrm{o}} \times \boldsymbol{F}_{\mathrm{n,o}} = 0 \,. \tag{66}$$

Provided the shanks of both legs are parallel to each other, equation (65) implies

$$\boldsymbol{F}_{\mathrm{n,i}} = -a\boldsymbol{F}_{\mathrm{g,eff}} \quad \text{and} \quad \boldsymbol{F}_{\mathrm{n,o}} = (a-1)\boldsymbol{F}_{\mathrm{g,eff}} \,,$$

where $0 \leq a \leq 1$. Substituting these into equation (66), we obtain

$$\boldsymbol{F}_{\mathrm{g,eff}} \times (a\boldsymbol{r}_{\mathrm{i}} + (1-a)\boldsymbol{r}_{\mathrm{o}}) = 0$$

and hence

$$\boldsymbol{F}_{\mathrm{g,eff}} = A(\boldsymbol{r}_{\mathrm{o}} + a(\boldsymbol{r}_{\mathrm{i}} - \boldsymbol{r}_{\mathrm{o}})) \,.$$

Thus in balanced stance, $\boldsymbol{F}_{\mathrm{g,eff}}$ points to the inner edge of the outside ski when $a = 0$, to the inner edge of the inside ski when $a = 1$ and to somewhere in between when $0 < a < 1$. Since $a > 0$ implies $\Phi < \Psi$, the effect of loading of the inside ski is similar to the effect of the angulation. In particular, the upper speed limit is reduced compared to the case where only the outside ski is loaded. In order to ski in balance at speeds exceeding this reduced speed limit, the loading of the inside ski should decrease, $a \to 0$.

Discussion and Implications

In this paper we described a simple mathematical model of balanced carving turns in alpine skiing, which can be applied to snowboarding as well. The model combines a system of ordinary differential equations governing the CM motion with the so-called Ideal Carving Equation (ICE), which emerges from the analysis of the

skier balance in the frontal plane. ICE relates the local radius of the CM trajectory to skier's speed and direction of motion relative to the fall line and hence provides closure to the system.

In the case of fall-line gliding, the skier speed grows until the gravity force is balanced by the aerodynamic drag and snow friction forces. Unless the slope is of very low gradient, the snow friction is a minor factor and can be ignored, whereas the balance between the gravity and the aerodynamic drag yields the saturation speed V_{g}. For this reason, V_{g} and the distance L_{g} required to reach it could be considered as the characteristic scales of alpine skiing. However, in the case of balanced carving turns, ICE introduces another characteristic speed, the carving speed limit V_{sc}. When the skier speed exceeds V_{sc}, the balance of forces acting on the skier can no longer be sustained. Because as a rule V_{sc} is lower than V_{g}, this suggests that V_{sc} is more relevant in the dynamics of carving turns. Moreover, the radius of carving turns cannot exceed the ski sidecut radius R_{sc}, making the latter a natural length scale of this dynamics. These two scales lead to the dimensionless equations of carving turn which have only three dimensionless control parameters: the slope gradient angle α, the dynamic coefficient of friction μ and the dynamic sidecut parameter $\mathrm{K} = R_{\mathrm{sc}}/L_{\mathrm{g}}$, which appears as a coefficient of the term, Kv^2, describing the aerodynamic drag force.

We used the model to explore ski runs composed of linked carving turns on a slope with constant gradient. While in reality such turns are linked via a transition phase of finite duration, in our simulations the transitions are instantaneous and take place at a specified traverse angle (the angle between the skier trajectory and the fall line). At the transition, the skier speed and direction of motion remain invariant, whereas the inclination angle and hence the turn radius jump to the values corresponding to the next turn. Under these conditions, the solution either approaches a limit cycle, where the turns become indistinguishable one from another, or terminates after reaching the speed limit V_{sc}.

When measured in the units of R_{sc} and V_{sc}, the balanced carving solutions corresponding to 13m $< R_{\mathrm{sc}} <$ 50m are rather similar. This is because 1) R_{sc} enters the problem only via the dynamic sidecut parameter $\mathrm{K} = R_{\mathrm{sc}}/L_{\mathrm{g}} \ll 1$ which determines the relative strength of the aerodynamic drag force, and 2) for $V < V_{\mathrm{sc}}$ this force remains relatively small. Yet the drag term is not entirely negligible and the solutions show some mild variation with R_{sc}. In particular, turns corresponding to a larger sidecut radius are less extreme, with smaller inclination angles and weaker g-forces.

Our results show the existence of a critical slope angle $\alpha_{\mathrm{c,t}}$ above which the speed of balanced ideal carving run eventually exceeds V_{sc}. The value of $\alpha_{\mathrm{c,t}}$ depends on the coefficient of friction μ and to a lesser degree on the sidecut parameter of the skis. For $\mu = 0.04$ we find $\alpha_{\mathrm{c,t}} = 17°$ for SL skis, $19°$ for GS skis and $21°$ for DH skis. In practice, a number of factors, such as the hardness of snow, structural integrity of skis and strength of human body, come into play well before this theoretical limit and

restrict balanced carving to slopes of even lower gradient. For example, demanding that the skier inclination angle remains below $\Phi_c = 70°$ (and hence the g-force below three), we find that for SL skis the critical inclination angle $\alpha_c \approx 9°$ if $\mu = 0.04$ and $\alpha_c \approx 16°$ if $\mu = 0.1$. For DH skis the corresponding values are $\alpha_c \approx 14°$ and $21°$. Overall, we find that the critical gradient increases linearly with μ.

Slopes of sub-critical gradient can be roughly divided into the gentle and moderately steep groups. For slopes of gentle gradient (aka "flat slopes"), the aerodynamic drag is not dominant over the snow friction even in the case of fall-line gliding and in carving runs the turn speed saturates well below both V_g and V_{sc}. The carved arcs are nearly circular and their radius is only slightly below the sidecut radius of the skis. The skier inclination angle and the g-force stay relatively small.

On slopes of moderate gradient the saturation speed of fall-line gliding is close to V_g, which is significantly above V_{sc}. However, the speed of carving runs saturates near V_{sc}, mostly because of the frictional energy losses. The closeness to the speed limit makes the carving turns quite extreme. Their shape deviates from the rounded shape of the letter C and reminds the letter J instead, with the local turn curvature significantly increasing on the approach to the fall line. As the curvature increases, the centrifugal force and hence the total g-force experienced by the skier grow. In order to stay in balance, they have to adopt large inclination to the slope. The significantly increased effective gravity leads to high normal reaction from the snow and hence significantly increased friction, which is the reason why the speed stays well below V_g.

On slopes of super-critical gradient ($\alpha > \alpha_c$) the speed quickly exceeds V_{sc}, after which the balanced carving cannot be continued.

The fact that balanced carving requires ski slopes to be rather gentle (of the green gradient in the US colour-coding scheme) is interesting as most slopes of ski resorts are steeper, not to mention typical race tracks. In conflict with this, skillful skiers manage to execute on such slopes at least partly carved turns. One possible explanation is that they use the skidding phase of their hybrid turns to slow down and keep their speed below V_{sc}. This may be true for recreational skiers but not so for top racers in competitive runs. In Table 1 we show average speeds achieved in FIS World Cup races (Gilgien, Crivelli, Spörri, Kröll, & Müller, 2015; Gilgien et al., 2014; Supej et al., 2014) as well as the speed limit V_{sc} calculated using equation (40), which can be written in the following convenient form:

$$V_{sc} = 40 \left(\frac{R_{sc}}{13\,\mathrm{m}} \right)^{1/2} \left(\frac{\cos \alpha}{\cos 15°} \right)^{1/2} \mathrm{km\,h}^{-1} . \tag{67}$$

One can see that in all the disciplines, the average racer speed exceeds the upper speed limit of balanced carving. Obviously, on fast sections of race course the conflict is even stronger. For example, in downhill competitions the current speed record is $v = 162\,\mathrm{km\,h}^{-1}$ (racer Johan Clarey, Wengen track). This comparison shows that the restrictions set by the theory of balanced pure carving are not consistent with the

Table 1
Parameters of race runs (Gilgien et al., 2015, 2014; Supej et al., 2014). R_{sc} is the sidecut radius of skis, α is the inclination angle of the slope, $\langle L_v \rangle$ and $\langle L_h \rangle$ are the mean separations between the gates down the fall line and across the fall line, respectively, R_a is the radius of the arc defined by the mean gate separations, V is the skier speed, $\zeta = \langle V \rangle^2 / g R_{sc}$ is a dimensionless speed parameter and L_g is the distance along the fall line required to reach the speed $\langle V \rangle$.

Parameter	SL	GS	SG	DH
$\langle \alpha \rangle$ [°]	20	18 ± 7	17 ± 7	14 ± 8
R_{sc} [m]	≤ 15	27	33	45
$R_{\min}$ [m]	7	8.4	17.2	20.6
$\langle V \rangle$ [km/h]	45	62	82	86
V_{sc} [km/h]	43	57	63	75

practice of alpine ski racing and some of the assumptions made in the theory are not quite valid and require critical examination.

One of the most obvious weaknesses of the model is that it cannot describe self-consistently the transition phase between carving turns. Such a transition does not arise naturally as a part of the solution of differential equations. Instead, it is introduced somewhat arbitrary as a link between two different solutions describing two different arcs of balanced carving. If the solution describing an arc is not terminated, the arc will continue uphill until the skier stops. The reason for this is that in the transition a skier cannot not be in balance and hence one has to go beyond the assumption of balanced carving in order to deal with it.

Even the modelling of a single turn is not entirely self-consistent. On the one hand, the model assumes that at every point of the turn the total torque acting on the skier vanishes. On the other hand, the balance condition yields the skier inclination that varies throughout the turn, which can only be the case if the torque does not vanish. This shows that in reality the balance can be only approximate. The model may still be relevant provided the characteristic time of reaching balance is much shorter that the turn duration but in order to verify this condition a more advanced theory is required.

Our analysis of the case with $v > V_{\mathrm{sc}}$ shows that for such high speeds the net torque pushes skier upwards, towards the position perpendicular to the slope, no matter what the skier inclination to the slope is. In other words, the centrifugal force always dominates gravity. This suggests that in this regime the dynamics of skier's body may be similar to that of a pendulum, with its natural oscillations about the vertical position.

Another obvious fact is that the typical speed of even elite racers is much lower than the limit set by the drop of potential energy and air resistance. As the wet snow friction is very low, this implies another channel of energy dissipation which is not

included in our model but plays a key role in the dynamics of a typical ski turn. As we have stated in the introduction, the typical turn is hybrid in nature and involves a significant degree of skidding in its initial phase. The high effective coefficient of friction associated with skidding (Sahashi & Ichino, 1998) shows that the skidding phase is most likely to be responsible for most of the energy dissipation in hybrid turns.

Conclusion

In this paper we explored in detail the model of carving turns in alpine skiing and snowboarding based on the usual assumption of approximate balance between forces and torques acting on the skier during the turn. In its basic form the model was proposed by Jentschura and Fahrbach (2004), where it was implicitly assumed that the skier was stacked and only one of the skis was loaded. We confirm the conclusion of Jentschura and Fahrbach (2004) that the approximation of torque balance yields an upper limit on the skier speed and show that it imposes a lower limit as well, with both these limits depending only on the sidecut radius of skis and the slope gradient. We use the model to simulate carving runs on slopes of constant gradient and find that in this model carving is possible only on relatively flat slopes, with the critical slope angle in the range of $8° - 20°$. The exact value depends mostly on the coefficient of snow friction and to a lesser degree on the sidecut radius of skis. We have extended the analysis to the case of an angulated skier and the case where both skis are loaded and found that in these cases the upper limits on the skier speed and the slope gradient are even more restrictive. This is in conflict with the practice of ski racing which demonstrates that carving is possible at higher speeds and on steeper slopes than the model allows. Our analysis of the torques exerted by the gravity and centrifugal forces shows that when the skier speed exceeds the upper limit of balanced carving, the lifting torque due to centrifugal force wins over the lowering torque of the gravity for any inclination angle of the skier. This suggests the possibility of carving runs where skiers swing from one side to another without settling to an equilibrium at any point of the turn, like a pendulum. A more advanced theory is needed to assess this hypothesis.

Acknowledgments

Appendix A
Edge radius of flexed skis

Here we analyse the geometry of a carving ski and how it changes when placed at the edge angle Ψ to a flat surface, which we assume to be hard and hence not changed in the process apart from a small cut possibly made in it by the ski's sharp steel

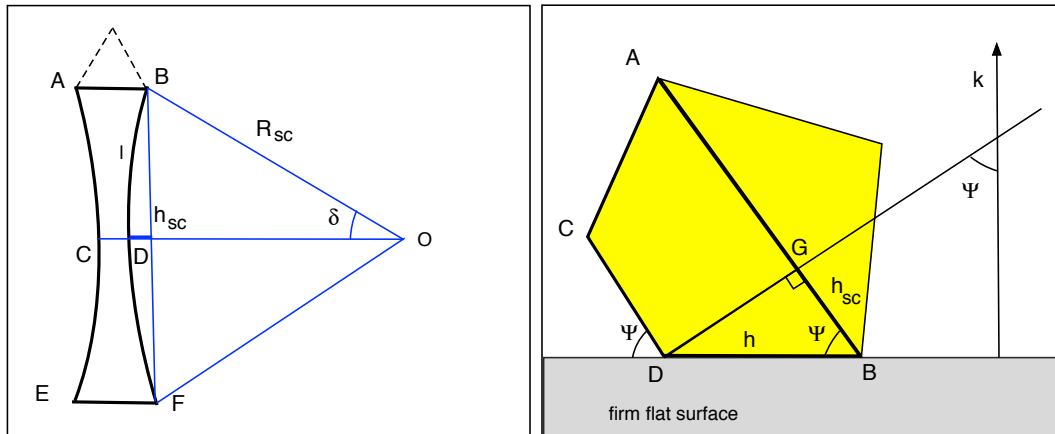*Figure A1*. *Left panel*: Shaped ski, its sidecut h_{sc} and sidecut radius R_{sc}. The dashed line shows the ski tip which is not important for determining R_{sc}. *Right panel*: The same ski with the edge BDF pressed against a hard flat surface at the edge angle Ψ as seen in projection on the plane normal to the ski at its waist. In this projection, DGB is a right-angle triangle.

edges. We start with the case where the ski lays flat as shown in the left panel of figure A1. In the figure, the ski is highly symmetric with no difference between its nose and tail sections. Although the real skis are wider at the nose this does not matter as long as their running edges can be approximated as circular arcs of radius R_{sc}, called the sidecut radius. Denote as D the point in the middle of the edge BF and as l the distance between B and D (or A and C) along the edge. As seen in this figure, $l = R_{sc}\delta$, where δ is the angular size of the edge DB as seen from its centre of curvature. This angle is normally rather small. For an SL ski of length $l_{ski} \approx 2l = 1.65\,\text{m}$ and $R_{sc} = 12.7\,\text{m}$ we have $\delta \approx 0.065$ (3°.7). For other kinds of racing skis, it is even smaller. The sidecut depth h_{sc} is defined as the distance between D and the straight line BF connecting the opposite ends of the edge. Obviously,

$$h_{sc} = R_{sc}(1 - \cos\delta)\,. \tag{68}$$

Using the first two terms of the Maclaurin expansion for $\cos\delta$

$$\cos\delta = 1 - \frac{1}{2}\delta^2 + O(\delta^4)$$

and then substituting $\delta = l/R_{sc}$ one finds the approximation

$$h_{sc} \simeq \frac{l^2}{2R_{sc}}\,. \tag{69}$$

Now suppose that this ski is kept at the angle Ψ to a firm flat surface and that it is pressed in the middle until its lower edge comes into the contact with the

surface along its whole length (excluding the tip). In this position the edge can still be approximated as an arc but a different one. Denote its radius as R_e and its "sidecut" depth as h (see the right panel of figure A1). Obviously R_e and h are connected in the same way as R_{sc} and h_{sc}

$$h = R_e(1 - \cos\delta)\,. \tag{70}$$

where now $\delta = l/R_e$. When $\delta \ll 1$, this is approximated as

$$h \simeq \frac{l^2}{2R_e} \tag{71}$$

and hence

$$\frac{R_e}{R_{sc}} = \frac{h_{sc}}{h}\,. \tag{72}$$

Analysing the right angle triangle GDB of the right panel in figure A1, one finds that $h_{sc} = h\cos\Psi$ and hence

$$\frac{R_e}{R_{sc}} = \cos\Psi\,. \tag{73}$$

This is the same as equation (9-4) in Howe (1983) and equation (3.7) in Lind and Sanders (1996).

Appendix B
Lateral stability

Here we analyse the stability of skier's balanced position in the transverse plane, focusing on the simplified case of loading only the outside ski.

We first consider the stability of a stacked skier. Suppose that in the equilibrium position the ski edge angle and the inclinations angle of the skier are Ψ_0 and $\Phi_0 = \Psi_0$ respectively. Hence,

$$\tan\Psi_0 = (\xi_0^2 - 1)^{1/2}\,, \quad \tan\Phi_0 = a\xi_0 + b\,, \tag{74}$$

where ξ_0 stands for the equilibrium turn radius. Consider a perturbation that changes the ski angulation position but keeps the skier velocity unchanged (and hence a and b as well). However, the turn radius changes and so does the effective gravity. We need to determine if the modified effective gravity is a restoring force or ti pushes the system further away from the equilibrium. In the perturbed state $\Psi = \Psi_0 + \delta\Psi$, $\Psi = \Phi_0 + \delta\Phi$ and $\xi = \xi_0 + \delta\xi$, where δA stands for the perturbation of A. It is clear that when $\delta\Psi > 0$ the instability condition reads $\Psi > \Phi$ or $\delta\Psi > \delta\Phi$, whereas for $\delta\Psi > 0$ it is $\delta\Psi < \delta\Phi$. Both these cases are captured in the instability condition

$$\frac{\delta\Phi}{\delta\Psi} < 1\,. \tag{75}$$

Using equation (74) we find

$$\delta(\tan\Psi) = \frac{\xi_0}{\tan\Psi_0}\delta\xi\,, \tag{76}$$

and

$$\delta(\tan\Phi) = a\delta\xi\,. \tag{77}$$

Hence,

$$\frac{\tan\delta\Phi}{\tan\delta\Psi} = \frac{a\tan\Psi_0}{\xi_0} = a\sin\Psi_0\,. \tag{78}$$

According to the condition (40), in carving turns $a < 1$ and hence equation (78) immediately yields $\tan\delta\Phi/\tan\delta\Psi < 1$. This implies $\delta\Phi/\delta\Psi < 1$ and therefore we conclude the lateral equilibrium is unstable.

While the balance of an angulated skier is still unstable, in this case there is an additional way of controlling the instability, namely by a suitable change of the angulation. If $\delta\Psi$ is the perturbation of the ski edge angle and $\delta\Phi$ is the corresponding perturbation of the effective gravity angle that the skier can restore their balance via changing their angulation by the amount

$$\delta\psi = \delta\Psi - \delta\Phi\,. \tag{79}$$

References

Brown, C. (2009). Modeling edge-snow interactions using machining theory. In E. Müller, L. S., & T. Stöggl (Eds.), *Science and skiing iv* (p. 175-182). Maidenhead, UK: Meyer & Meyer Sport.

Colbeck, S. (1992). *A review of the processes that control snow friction* (Tech. Rep.). Hanover, NH: Cold Regions Research and Engineering Laboratory (CRREL). Retrieved from `https://apps.dtic.mil/sti/citations/ADA252362`

Federolf, M., Lüthi, P., Roos, A., & Dual, J. (2010). Parameter study using a finite element simulation of a carving alpine ski to investigate the turn radius and its dependence on edging angle, load, and snow properties. *Sports Eng.*, *12*, 135-141.

Federolf, P., Roos, M., Lüthi, A., & Dual, J. (2010). Finite element simulation of the ski-snow interaction of an alpine ski in a carved turn. *Sports Engineering*, *12*, 123-133.

Gilgien, M., Crivelli, P., Spörri, J., Kröll, J., & Müller, E. (2015). Characterization of course and terrain and their effect on skier speed in world cup alpine ski racing. *PLoS ONE*, *10*, e0118119.

Gilgien, M., Spörri, J., Kröll, J., Crivelli, P., & Müller, E. (2014). Mechanics of turning and jumping and skier speed are associated with injury risk in men's world cup alpine skiing: a comparison between the competition disciplines. *British Journal of Sports Medicine*, *48*, 742-747.

Harb, H. (2006). *Essentials of skiing.* New York: Hatherleigh Press.

Hirano, Y. (2006). Quickest descent line during alpine ski racing. *Sports Eng.*, *9*, 221.

Howe, J. (1983). *Skiing mechanics.* Laporte, Colorado: Poudre Press.

Jentschura, U., & Fahrbach, F. (2004). Physics of skiing: The ideal carving equation and its applications. *Canadian Journal of Physics*, *82*, 249.

Landau, L., & Lifshitz, E. (1969). *Mechanics.* Oxford: Pergamon Press.

LeMaster, R. (2010). *Ultimate skiing.* Champaign: Human Kinetics.

Lind, D., & Sanders, S. (1996). *The physics of skiing: Skiing at the triple point.* New York: Springer-Verlag.

Merchant, M. (1945). Mechanics of the metal cutting process. i. orthogonal cutting and a type 2 chip. *J. Appl. Phys.*, *16*, 267-275.

Mössner, M., Heinrich, D., Kaps, P., Schretter, H., & Nachbauer, W. (2008). Computer simulation of consecutive ski turns. *Journal of ASTM International*, *5(8)*, 1.

Mössner, M., Heinrich, D., Kaps, P., Schretter, H., & Nachbauer, W. (2009). Efects of ski stiffness in a sequence of ski turns. In E. Müller, L. S., & S. T. (Eds.), *Science and skiing iv* (p. 374). Waterford, Maine: McIntire Publishing.

Mössner, M., Heinrich, D., Schindelwig, K., Kaps, P., Lugner, P., Schmiedmayer, H.-B., ... Nachbauer, W. (2006). Modeling of the ski-snow contact for a carved turn. In E. Moritz & S. Haake (Eds.), *Engineering of sport 6* (p. 195). New York: Springer.

Mössner, M., Innerhofer, G., Schindelwig, K., Kaps, P., Schretter, H., & Nachbauer, W. (2013). Measurement of mechanical properties of snow for simulation of skiing. *J.Glaciology*, *59*, 1170-1178.

Nachbauer, W., Kaps, P., Hasler, M., & Mössner, M. (2016). Friction between ski and snow. In F. Braghin, C. F., S. Maldifassi, & S. Melzi (Eds.), *The engineering approach to winter sports* (p. 33). New York: Springer.

Nordt, A., Springer, G., & Kollár, L. (1999). Simulation of a turn on alpine skis. *Sports Engineering*, *2*, 181-199.

Oberegger, U., Kaps, P., Mössner, M., Heinrich, D., & Nachbauer, W. (2010). Simulation of turns with a 3d skier model. *Procedia Engineering*, *2(2)*, 3171-3177.

Reid, R. (2010). *A kinematic and kinetic study of alpine skiing technique in slalom.* PhD dissertation, Norwegian School of Sport Sciences. Retrieved from `http://hdl.handle.net/11250/171325`

Reid, R. C., Haugen, P., Gilgien, M., Kipp, R. W., & Smith, G. A. (2020). Alpine ski motion characteristics in slalom. *Frontiers in Sports and Active Living*, *2*, 25. Retrieved from `https://www.frontiersin.org/article/10.3389/fspor.2020.00025` doi: 10.3389/fspor.2020.00025

Rudakov, R., Lisovski, A., Ilyalov, O., & Podgaets, R. (2010). Optimisation of the skier's trajectory in special slalom. *Procedia Engineering*, *2*, 3179-3182.

Sahashi, T., & Ichino, S. (1998). Coefficient of kinetic friction of snow skis during turning descents. *Japanese Journal of Applied Physics*, *37*, 720-727.

Spörri, J., Kröll, J., Gildien, M., & Müller, E. (2016). Sidecut radius and the mechanics of turning equipment designed to reduce risk of severe traumatic knee injuries in alpine giant slalom ski racing. *Br. J. Sports Med.*, *50*, 14-19.

Supej, M., Hebert-Losier, K., & Holmberg, H.-C. (2014). Impact of the steepness of the slope on the biomechanics of world cup slalom skiers. *International Journal of Sports Physiology and Performance*, *10*, 361-368.

Tada, N., & Hirano, Y. (2002). In search of the mechanics of a turning alpine ski using snow cutting force measurements. *Sports Engineering*, *5*, 15-22.

Yoneyama, T., Scott, N., Kagawa, H., & Osada, K. (2008). Ski deflection measurement during skiing and estimation of ski direction and edge angle. *Sports Engineering*, *11*, 3-13.